

**Argonne National Laboratory**

**A STUDY OF CONVECTIVE  
MAGNETOHYDRODYNAMIC CHANNEL FLOW**

**by**

**Ralph M. Singer**

## LEGAL NOTICE

This report was prepared as an account of Government sponsored work. Neither the United States, nor the Commission, nor any person acting on behalf of the Commission:

A. Makes any warranty or representation, expressed or implied, with respect to the accuracy, completeness, or usefulness of the information contained in this report, or that the use of any information, apparatus, method, or process disclosed in this report may not infringe privately owned rights; or

B. Assumes any liabilities with respect to the use of, or for damages resulting from the use of any information, apparatus, method, or process disclosed in this report.

As used in the above, "person acting on behalf of the Commission" includes any employee or contractor of the Commission, or employee of such contractor, to the extent that such employee or contractor of the Commission, or employee of such contractor prepares, disseminates, or provides access to, any information pursuant to his employment or contract with the Commission, or his employment with such contractor.

ARGONNE NATIONAL LABORATORY  
9700 South Cass Avenue  
Argonne, Illinois 60440

A STUDY OF CONVECTIVE  
MAGNETOHYDRODYNAMIC CHANNEL FLOW

by

Ralph M. Singer

Reactor Engineering Division

March 1965

Operated by The University of Chicago  
under  
Contract W-31-109-eng-38  
with the  
U. S. Atomic Energy Commission





## TABLE OF CONTENTS

	<u>Page</u>
NOMENCLATURE . . . . .	6
I. INTRODUCTION. . . . .	7
II. PREVIOUS WORK. . . . .	7
III. ANALYSIS. . . . .	8
A. Development of Equations . . . . .	8
B. Parallel-plate Channel . . . . .	13
1. Relationship of Pressure Drop to Flow Rate . . . . .	15
2. Heat Transfer Results . . . . .	15
3. Discussion of Results for Parallel-plate Channel . . . . .	16
C. Solution for Small Values of the Magnetic Prandtl Number . . . . .	21
1. Relationship of Pressure Drop to Flow Rate . . . . .	22
2. Heat Transfer . . . . .	22
3. Discussion of Results for Rectangular Channels . . . . .	23
D. Nonconducting Channel Walls. . . . .	26
1. Pressure Drop Parameter . . . . .	29
2. Heat Transfer Results . . . . .	29
3. Results and Discussion . . . . .	29
IV. CONCLUSIONS. . . . .	29
APPENDICES	
A. Fully-developed Assumption . . . . .	31
B. Parallel-plate Case Results . . . . .	34
1. Detailed Solutions . . . . .	34
2. Relationship of Pressure Gradient to Flow Rate . . . . .	35
3. Nusselt Numbers . . . . .	35
4. Integration Constants. . . . .	37
C. Nonconducting Wall Case Results . . . . .	39
1. Detailed Solutions . . . . .	39
2. Pressure-drop Parameter . . . . .	40
3. Nusselt Number . . . . .	41
4. Integration Constants. . . . .	42
ACKNOWLEDGMENTS . . . . .	44
REFERENCES . . . . .	45

## LIST OF FIGURES

<u>No.</u>	<u>Title</u>	<u>Page</u>
1.	Cross-sectional Diagram of Channel . . . . .	10
2.	Effect of the Hartmann and Rayleigh Numbers on $G_{\infty}$ (Parallel-plate Channel) . . . . .	16
3.	Effect of the Hartmann and Rayleigh Numbers on the Nusselt Number (Parallel-plate Channel). . . . .	17
4.	Nusselt Number Ratio Variation with the Hartmann and Rayleigh Numbers (Parallel-plate Channel). . . . .	18
5.	Map of the M-Ra Plane Showing Region of Free-convection Importance (Parallel-plate Channel) . . . . .	18
6.	Effect of the Wall Conductance Ratio and Hartmann Number on $G_{\infty}$ (Parallel-plate Channel) . . . . .	19
7.	Effect of Internal Energy Generation on $G_{\infty}$ (Parallel-plate Channel) . . . . .	20
8.	Effect of Internal Energy Generation on the Nusselt Number (Parallel-plate Channel) . . . . .	20
9.	Velocity Profile Variation with the Hartmann Number (Small $Pr_m$ Case) . . . . .	23
10.	Temperature Profile Variation with the Hartmann Number (Small $Pr_m$ Case). . . . .	23
11.	Effect of the Aspect Ratio and Hartmann Number on a Flow Rate Ratio (Small $Pr_m$ Case) . . . . .	24
12.	Map of M- $\gamma$ Plane Showing Region of Two-dimensional Effects (Small $Pr_m$ Case) . . . . .	25
13.	Effect of the Aspect Ratio and Hartmann Number on the Nusselt Number (Small $Pr_m$ Case) . . . . .	25







## NOMENCLATURE

English  
Letters

$a$	Half-width of channel
$a_m$	Fourier coefficient
$A$	Temperature gradient, defined in equation (21)
$b$	Half-breath of channel
$B_2$	Form of $B$ , defined in Appendix C
$\underline{B}$	Magnetic flux density vector
$B$	Dimensionless magnetic flux density, $B = B_x/B_0C$
$c$	Heat capacity
$C$	Parameter defined as $(a^3c/\nu k)/[-(\partial p/\partial x) - \rho g]$
$C^*$	Parameter defined as $(a^3c/\nu k)/[-(\partial p/\partial x) - \rho g + \sigma B_0 E_0]$
$\underline{D}$	Dielectric displacement vector
$\underline{E}$	Electric field intensity vector
$F$	Internal energy generation index, $F = Qa/kAC$
$F^*$	Internal energy generation index, $F^* = Qa/kAC^*$
$\underline{g}, \underline{g}$	Gravitational acceleration magnitude, vector
$C_w, G^*$	Ratio of mean flow rate to pressure gradient, defined in equations (42) and (62)
$h$	Thickness of channel walls
$\underline{H}$	Magnetic field strength vector
$\underline{J}$	Current density vector
$k$	Thermal conductivity
$M$	Hartmann number, $aB_0(\sigma/\mu)^{1/2}$
$\underline{n}^*$	Outward normal
$m, n$	Summation indices
$Nu$	Nusselt number, $(q_w \cdot 2a)/[k(T_w - T_B)]$
$Pr$	Thermal Prandtl number, $\rho \nu c/k$
$Pr_m$	Magnetic Prandtl number, $\sigma \mu_0 \nu$
$p_1, p_2, p_3$	Quantities defined in Appendix C
$p_1(x, z)$	Pressure function defined in equation (A2)
$p, p(x, y, z)$	Pressure
$p_2(y, z)$	Pressure function defined in equation (A14)
$q$	Heat Flux
$q_1, q_2, q_3$	Quantities defined in Appendix C
$Q$	Internal volumetric energy generation rate
$Ra$	Rayleigh number, $Ra = g \beta \rho c a^4 A / \nu k$
$R_m$	Magnetic Reynolds' number, $R_m = \mu_0 \sigma a \bar{u}$
$t$	Time
$T, T_B$	Temperature, bulk fluid temperature
$T_1, T_2$	Temperature defined in equation (A7)
$u$	Local velocity in x-direction
$\bar{u}$	Mean velocity in x-direction
$U$	Dimensionless form of $u$ , $U = apcu/kC$

$U^*$	Dimensionless form of $u$ , $U^* = apcu/KC^*$
$U_2$	Form of $U$ , defined in Appendix C
$\underline{V}$	Velocity field vector
$x, y, z$	Rectangular coordinates

Greek  
Letters

$\alpha_i, i = 1 \text{ to } 6$	Integration constants defined in Appendix C
$\beta$	Thermal expansion coefficient
$\gamma$	Aspect ratio, $b/a$
$\epsilon_0$	Inductive capacity
$\zeta$	Dimensionless form of $z$ , $\zeta = z/a$
$\eta$	Dimensionless form of $y$ , $\eta = y/a$
$\theta$	Dimensionless temperature difference, $\theta = (T - T_w)/aAC$
$\theta^*$	Dimensionless temperature difference, $\theta^* = (T - T_w)/aAC^*$
$\theta_2$	Form of $\theta$ , defined in Appendix C
$\kappa, \kappa', \kappa_i$	Integration constants
$\lambda_i$	Parameters defined in Appendix B
$\mu$	Dynamic viscosity
$\mu_0$	Magnetic permeability
$\nu$	Kinematic viscosity
$\rho$	Mass density
$\rho_e$	Charge density
$\sigma$	Electrical conductivity
$\phi$	Viscous and ohmic dissipation term
$\phi, \phi_1, \phi_2$	Wall electrical conductance ratios
$\omega_i, i = 1 \text{ to } 5$	Integration constants defined in Appendix C

## Subscripts

$mn$	Double Fourier transform
$m \text{ or } n$	Single Fourier transform
$m_1$	Single Fourier transform for $m < m_0$
$m_3$	Single Fourier transform for $m > m_0$
$w$	Wall conditions
$x, y, z$	Scalar component of vector in $x, y, z$ direction
$0$	Applied value
$\infty$	Parallel-plate case

## Superscript

$*$	Small magnetic Prandtl number case
-----	------------------------------------



# A STUDY OF CONVECTIVE MAGNETOHYDRODYNAMIC CHANNEL FLOW

by

Ralph M. Singer

## I. INTRODUCTION

If a magnetohydrodynamic device (e.g., a MHD power generator, or an electromagnetic pump) is to be intelligently designed, information must be available concerning the effects of the interactions of the electromagnetic, velocity, and temperature fields. In the past, a great analytical effort has been extended to understand the velocity and electromagnetic interactions; however, little has been done with thermal interactions. This is understandable, since in nonconvective flow (no natural convective forces), the energy equation is uncoupled from Maxwell's equations and the Navier-Stokes equations. Thus, the electromagnetic and velocity fields can be determined independently of the temperature field. However, when natural convective forces are present, the Navier-Stokes equations become coupled with the energy conservation equation, and simultaneous solution is required.

This report analyzes a class of steady magnetohydrodynamic channel flow problems when natural, as well as forced, convection is important. The analyses are restricted to cases of fully-developed laminar flow in vertical rectangular channels.

## II. PREVIOUS WORK

The purpose of this section is not to present a thorough review of the literature on MHD channel flow, but only to indicate briefly some of the more important work in this area.

Since the pioneer work of Hartmann<sup>(1)</sup> in 1937 in developing and analyzing the electromagnetic pump, many analyses of crossed-field devices have appeared in the literature. Hartmann studied the laminar, isothermal flow of an electrically-conducting fluid (mercury) between two infinite, parallel plates with a uniform, imposed magnetic field. The channel walls were assumed to be perfect nonconductors (zero electrical conductivity).

This work was extended by Shercliff<sup>(2,3)</sup> to the case of a finite channel. Shercliff also determined the asymptotic solutions for large values of the Hartmann number ( $Ba\sqrt{\sigma/\mu}$ ) and showed that the velocity

profile degenerates into a core of uniform flow surrounded by boundary layers on the walls. Shercliff's work on nonconducting channel walls was then extended to the case of perfectly-conducting channel walls by Uflyand<sup>(4)</sup> and finite conducting walls by Chekmarev.<sup>(5)</sup>

Chang and Lundgren<sup>(6,7)</sup> and Chang and Yen<sup>(8)</sup> then determined the effect of finite channel-wall conductivity on isothermal flow in parallel-plate channels. Yen<sup>(9)</sup> also solved the uncoupled energy equation for duct flow with electrically-conducting channel walls.

To the knowledge of the author, the first analysis of natural, convective, MHD channel flow was made by Smirnov<sup>(10)</sup> in which a round, vertical tube with nonconducting walls was considered in an approximate fashion. A similar, more rigorous analysis for the case of a parallel-plate channel was presented by Poots,<sup>(11)</sup> again for nonconducting channel walls. Poots also studied the case of natural convective flow set up by Joule heating in a circular tube. Osterle and Young<sup>(12)</sup> determined the role of viscous and Joule dissipation on the free-convection temperature and velocity profiles in a parallel-plate channel.

Combined natural and forced convective flow in nonconductive channels with transverse magnetic fields was analyzed by Mori<sup>(13)</sup> and Regirer.<sup>(14,15)</sup> Mori restricted his analysis to a parallel-plate channel, while Regirer<sup>(15)</sup> considered a vertical tube but did not present any numerical results. Regirer<sup>(14)</sup> also presented a solution for the parallel-plate case but again did not calculate any numerical results.

Many analyses have been made of forced convection in channels with a transverse magnetic field. The parallel-plate channel was analyzed by Alpher<sup>(16)</sup> (electrically-conducting walls) and Perlmutter and Siegel<sup>(17)</sup> (nonconducting walls), and the annular channel by Shohet<sup>(18)</sup> and Globe.<sup>(19)</sup> The case of flow and heat transfer on external surfaces will not be discussed here.

This review of the literature indicates that no analyses are available that consider combined convective flow in finite channels with electrically-conducting walls. This report will present such an analysis. The previously-published results will be shown to be special cases of this more general treatment of the problem.

### III. ANALYSIS

#### A. Development of Equations

To describe mathematically the convective flow of an electrically-conducting fluid through an electromagnetic field, one must employ Maxwell's (electromagnetic) equations, Ohm's law, the modified Navier-Stokes equations,



and the energy conservation equation. Since there are mechanical forces of electrical origin (electromotive force) and of magnetic origin (magnetomotive force), and electric effects of mechanical origin (induced emf), as well as mechanical effects of thermal origin (thermally induced buoyancy), it is expected that the equations describing convective flow will be coupled. In other words, simultaneous solution of the descriptive equations will be necessary.

As has been shown by many authors (e.g., reference 20), the Maxwell field equations may be written as

$$\nabla \times \underline{E} = -\frac{\partial \underline{B}}{\partial t}, \quad (1)$$

$$\nabla \times \underline{H} = \underline{J} + \frac{\partial \underline{D}}{\partial t}, \quad (2)$$

$$\nabla \cdot \underline{B} = 0, \quad (3)$$

and

$$\nabla \cdot \underline{D} = \rho_e, \quad (4)$$

where

$$\underline{B} = \mu_0 \underline{H}, \quad \text{and} \quad \underline{D} = \epsilon_0 \underline{E}, \quad (5a, b)$$

and Ohm's law may be written as

$$\underline{J} = \sigma(\underline{E} + \underline{V} \times \underline{B}). \quad (6)$$

The subscript zero on  $\mu$  and  $\epsilon$  restricts the subsequent analysis to the exclusion of any ferromagnetic material, so that  $\mu_0$  and  $\epsilon_0$  are numerically equal to their respective values in a vacuum. Also, the electrical conductivity,  $\sigma$ , will be assumed to be a scalar (Hall effect neglected).

As shown by Elsasser,<sup>(21)</sup> in all practical forms of magnetohydrodynamics, the displacement current ( $\partial \underline{D} / \partial t$ ) is altogether negligible in comparison to  $\underline{J}$  (note that under steady conditions, the displacement current identically vanishes) and also, purely electrostatic effects (i.e., the charge density,  $\rho_e$ ) are negligible. Thus, equations (2) and (4) can be reduced to (using 5a, b)

$$\nabla \times \underline{B} = \mu_0 \underline{J}, \quad (2a)$$

and

$$\nabla \cdot \underline{E} = 0. \quad (4a)$$

The modified Navier-Stokes equations for incompressible flow can be written as

$$\rho \left[ \frac{\partial \underline{V}}{\partial t} + (\underline{V} \cdot \nabla) \underline{V} \right] = -\nabla P + \rho \nu \nabla^2 \underline{V} + \rho \underline{g} + \underline{J} \times \underline{B}, \quad (7)$$

where

$$\nabla \cdot \underline{V} = 0. \quad (8)$$

The term  $\underline{J} \times \underline{B}$  represents the force exerted on the fluid due to the electromagnetic interaction with the moving fluid. Also, the energy conservation equation is

$$\rho c \left( \frac{\partial T}{\partial t} + \underline{V} \cdot \nabla T \right) = k \nabla^2 T + Q + \Phi + \frac{1}{\sigma} (\underline{J} \cdot \underline{J}), \quad (9)$$

where  $Q$  is the internal energy generation,  $\Phi$  represents the viscous energy dissipation, and the last term is the ohmic heating effect.

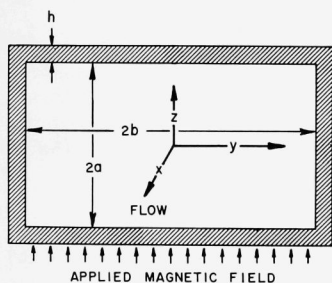


Fig. 1. Cross-sectional Diagram of Channel

The general problem considered in this report is the convective flow of an electrically- and thermally-conducting fluid in a vertical rectangular channel. A uniform magnetic field will be applied transverse to the flow (a schematic diagram of the channel and coordinate system is shown in Figure 1). Only the case of steady, laminar, fully-developed flow and heat transfer will be considered. This implies that all physical quantities (except possibly pressure and temperature) are independent of  $x$ . Also, there can be no net current flow in the  $x$ -direction, and the velocity can have only an  $x$ -component.

Based on these assumptions, it can be shown<sup>(6)</sup> that  $\underline{B}$ ,  $\underline{E}$ , and  $\underline{J}$  must have the forms

$$\underline{B} = [B_x(y,z), 0, B_0], \quad (10)$$

$$\underline{E} = [0, E_y(y,z), E_z(y,z)], \quad (11)$$

and

$$\underline{J} = [0, J_y(y,z), J_z(y,z)], \quad (12)$$

where  $B_0$  is the constant applied magnetic field strength. Thus, equations (1) through (6) reduce to

$$J_y = \frac{1}{\mu_0} \frac{\partial B_x}{\partial z} = \sigma(E_y - uB_0), \quad (13a,b)$$

$$J_z = -\frac{1}{\mu_0} \frac{\partial B_x}{\partial y} = \sigma E_z, \quad (14a,b)$$

and

$$\frac{\partial E_y}{\partial y} + \frac{\partial E_z}{\partial z} = \frac{\partial E_y}{\partial z} - \frac{\partial E_z}{\partial y} = 0, \quad (15a,b)$$

and equations (7), (8), and (9) reduce to

$$-\frac{\partial p}{\partial x} + \rho \nu \left( \frac{\partial^2 u}{\partial z^2} + \frac{\partial^2 u}{\partial y^2} \right) - \rho g + J_y B_0 = 0, \quad (16)$$

$$-\frac{\partial p}{\partial y} + J_z B_x = 0, \quad (17)$$

$$-\frac{\partial p}{\partial z} - J_y B_x = 0, \quad (18)$$

and

$$\rho c u \frac{\partial T}{\partial x} = k \left( \frac{\partial^2 T}{\partial x^2} + \frac{\partial^2 T}{\partial y^2} + \frac{\partial^2 T}{\partial z^2} \right) + Q, \quad (19)$$

where ohmic and viscous dissipation have been neglected in (19).

Combining equations (15b), (13b), and (14b) yields the following equation showing the interdependence of velocity and induced magnetic field:

$$\frac{\partial^2 B_x}{\partial y^2} + \frac{\partial^2 B_x}{\partial z^2} + \mu_0 \sigma B_0 \frac{\partial u}{\partial z} = 0. \quad (20)$$

The assumption that the flow and heat transfer are fully developed required that  $u = u(y, z)$ ; i.e., the velocity is unchanging along the length of the channel. It can be shown (see Appendix A for details) that as a result of this assumption, along with the conditions (10), (11), and (12), the pressure gradient in the  $x$ -direction,  $\partial p / \partial x$ , is required to be constant and the temperature is required to vary only linearly with  $x$ ; i.e.,

$$T(x, y, z) = Ax + T_2(y, z). \quad (21)$$

Note that equation (21) also implies that

$$T(x, y, z) - T_w(x) = \text{function of } y \text{ and } z \text{ only}. \quad (22)$$

Substituting equation (21) into equation (19) yields

$$\rho c \text{Au} = k \left( \frac{\partial^2 T_2}{\partial y^2} + \frac{\partial^2 T_2}{\partial z^2} \right) + Q. \quad (23)$$

Finally, if small density variations are allowed to occur because of temperature differences, the density in equation (16) can be expressed as

$$\rho \cong \rho_w - \beta \rho_w (T - T_w). \quad (24)$$

The equations that must now be solved to determine  $B_x$ ,  $u$ , and  $T$  are (16), (20), and (23), in conjunction with the relations (13a) and (24). The remaining equations are of secondary importance insofar as they are not needed in the determination of the magnetic, velocity, and temperature fields.

For convenience, the pertinent equations can be cast into dimensionless form by defining the quantities  $\eta$ ,  $\xi$ ,  $U$ ,  $\theta$ , and  $B$  (see nomenclature for definitions). There results

$$\nabla^2 U + \text{Ra} \theta + \left( \frac{M^2 \text{Pr}}{\text{Pr}_m} \right) \frac{\partial B}{\partial \xi} = -1, \quad (16a)$$

$$\nabla^2 \theta + F = U, \quad (22a)$$

and

$$\nabla^2 B + \left( \frac{\text{Pr}_m}{\text{Pr}} \right) \frac{\partial U}{\partial \xi} = 0, \quad (20a)$$

where

$$\nabla^2 = \partial^2 / \partial \eta^2 + \partial^2 / \partial \xi^2$$

and  $\text{Ra}$ ,  $M$ ,  $\text{Pr}$ ,  $\text{Pr}_m$ ,  $F$  are the Rayleigh, Hartmann, thermal Prandtl, magnetic Prandtl, and energy generation numbers, respectively.

The necessary boundary conditions on  $U$  and  $\theta$  are merely

$$\theta = U = 0 \quad \text{at } \eta = \pm \gamma, \xi = \pm 1, \quad (25a,b)$$

which state that the temperature of the fluid at the wall equals that of the wall and there is no fluid slip at the walls. The boundary conditions on  $B$  must be obtained from the electromagnetic conditions at the walls, which are (20)



(a) The tangential component of  $\underline{E}$  is continuous (no surface currents).

(b) The tangential and normal components of  $\underline{B}$  are continuous. From Shercliff<sup>(3)</sup> and Chang and Lundgren,<sup>(6)</sup> it is shown that the proper boundary conditions for thin walled ducts ( $h/a \ll 1$ ) are

$$\frac{\partial B}{\partial n^*} + \frac{B}{\phi} = 0 \quad \text{at walls,} \quad (26)$$

where  $n^*$  is an outward normal and  $\phi$  is defined as

$$\phi = \sigma_w h / \sigma_a,$$

where  $\sigma_w$  is the electrical conductivity of the wall. Letting  $\phi_1$  represent  $\phi$  at  $\eta = \pm\gamma$ , and  $\phi_2$  represent  $\phi$  at  $\zeta = \pm 1$ , condition (26) may be written as

$$\frac{\partial B}{\partial \zeta} \pm \frac{B}{\phi_2} = 0, \quad \text{at } \zeta = \pm 1; \quad (27)$$

and

$$\frac{\partial B}{\partial \eta} \pm \frac{B}{\phi_1} = 0, \quad \text{at } \eta = \pm\gamma. \quad (28)$$

The system of partial differential equations (16a), (22a), and (20a) with the boundary conditions (25a,b), (27), and (28) could not, in general, be analytically solved. Thus, several special cases will be considered in the remainder of this report.

## B. Parallel-plate Channel

If the aspect ratio of the channel,  $\gamma$ , is allowed to become very large, the differential system becomes one-dimensional, since all gradients in the  $\eta$ -direction become negligibly small in comparison to those in the  $\zeta$ -direction. Thus, the system reduces to

$$\frac{d^2 U_\infty}{d\zeta^2} + Ra\theta_\infty + \left( \frac{M^2 Pr}{Pr_m} \right) \frac{dB_\infty}{d\zeta} = -1, \quad (29)^*$$

$$\frac{d^2 \theta_\infty}{d\zeta^2} + F = U_\infty, \quad (30)$$

$$\frac{d^2 B_\infty}{d\zeta^2} + \left( \frac{Pr_m}{Pr} \right) \frac{dU_\infty}{d\zeta} = 0, \quad (31)$$

---

\*The subscript  $\infty$  refers to  $\gamma = \infty$ .

and

$$\text{at } \zeta = \pm 1, \quad \frac{dB_\infty}{d\zeta} \pm \frac{B_\infty}{\phi_2} = U_\infty = \theta_\infty = 0. \quad (32a,b,c)$$

The special case of  $\phi_2 = 0$  (nonconducting channel walls) has been solved by Regier<sup>(14)</sup> and Mori,<sup>(13)</sup> and the case of  $Ra = 0$  (no natural convection effects) has been solved by Yen.<sup>(9)</sup> Also, a similar problem with  $M = 0$  (no magnetic field present) was solved by Ostrach.<sup>(22)</sup> These solutions are all limiting cases of the one to be presented in this section.

To uncouple the differential system, (29)-(31) equation (31) is integrated once to yield

$$\frac{dB_\infty}{d\zeta} + \left( \frac{Pr}{Pr_m} \right) U_\infty = \left( \frac{dB_\infty}{d\zeta} \right)_{\zeta=-1} \equiv \kappa,$$

where  $\kappa$  is at present undetermined. Then, this expression for  $dB_\infty/d\zeta$  is substituted into equation (29). Finally, combining equations (29) and (30) results in

$$\frac{d^4 U_\infty}{d\zeta^4} - M^2 \frac{d^2 U_\infty}{d\zeta^2} + Ra U_\infty = Ra F. \quad (33)$$

The boundary conditions on  $U_\infty$  to be used are

$$U_\infty = \frac{d^2 U_\infty}{d\zeta^2} + \left( 1 + \frac{\kappa M^2 Pr_m}{Pr} \right) = 0 \quad \text{at } \zeta = \pm 1, \quad (34a,b)$$

and  $\theta$  and  $B$  are related to  $U$  by the relations

$$-Ra\theta_\infty = \frac{d^2 U_\infty}{d\zeta^2} - M^2 U_\infty + \left( 1 + \frac{\kappa M^2 Pr_m}{Pr} \right), \quad (35)$$

and

$$B_\infty = \int \left( \kappa - \frac{Pr_m}{Pr} U_\infty \right) d\zeta + \text{constant}. \quad (36)$$

Since the boundary conditions on  $\theta_\infty$  have been absorbed into those for  $U_\infty$ ,  $\theta_\infty$  may be directly obtained from the solution of  $U_\infty$ . However, the boundary conditions on  $B_\infty$  must still be involved in order to determine  $\kappa$  and the other constant in equation (36).

A study of the indicial equation corresponding to equation (33) reveals that the functional form of  $U(\xi)$  depends upon the relative magnitudes of  $M^4$  and  $4Ra$ . Thus, the forms of  $\theta$  and  $B$  also depend upon this criterion.

Since the solutions can be obtained by a straightforward, although tedious technique, only the final solutions will be presented, and they are shown in Appendix B.

### 1. Relationship of Pressure Drop to Flow Rate

From the solutions for the dimensionless velocity profile,  $U(\xi)$ , a relationship between the mass average velocity and the pressure drop can be obtained. The definition of the mass average velocity is just

$$\bar{u} = \left( \int_A u dA \right) / \left( \int_A dA \right), \quad A \sim \text{area}, \quad (41)$$

so that utilizing the dimensionless quantities previously defined, there results

$$\frac{\mu \bar{u}}{a^2 \left( -\frac{\partial P}{\partial x} - \rho g \right)} \equiv G_\infty = \frac{1}{2} \int_{-1}^{+1} U(\xi) d\xi. \quad (42)$$

This relationship yields the dependence of  $G_\infty$  upon the Rayleigh, Hartmann, Prandtl, magnetic Prandtl, energy generation, and wall conductance numbers. Using the velocity distributions from Appendix B, the integral in equation (42) can be evaluated, and the results are listed in Appendix B.

### 2. Heat Transfer Results

With the type of thermal boundary condition chosen in this analysis (uniform wall heat flux, or equivalently, linearly-varying wall temperature), a quantity of practical interest is the heat transfer coefficient based on the temperature difference between the wall and the "bulk" fluid. A knowledge of such a coefficient and the channel wall conditions would make it possible to easily calculate the bulk temperature of the fluid.

By definition, the bulk fluid temperature is

$$T_B = \left( \int_A u T dA \right) / \left( \int_A u dA \right). \quad (47)$$

Introducing the definitions of the dimensionless quantities  $\theta$ ,  $U$ , and  $\xi$  results in

$$\frac{2\rho\bar{u}c(T_B - T_W)}{kAC^2} = \int_{-1}^{+1} U_{\infty} \theta_{\infty} d\xi. \quad (48)$$

This relationship can be rephrased in terms of the Nusselt number, defined as

$$Nu_{\infty} = \left[ \frac{q_w \cdot 2a}{k(T_W - T_B)} \right], \quad (49)$$

so that equation (48) may be rewritten as

$$Nu_{\infty} = (F - G_{\infty}) \left( \frac{1}{2G_{\infty}} \int_{-1}^{+1} U_{\infty} \theta_{\infty} d\xi \right)^{-1}. \quad (48a)$$

From the expressions for  $U$  and  $\theta$ , it can be seen that  $Nu_{\infty}$  will be a function of the Rayleigh number,  $Ra$ , the Hartmann number,  $M$ , and the heat generation index,  $F$ . The integration can be carried out easily, and the results are shown in Appendix A.

### 3. Discussion of Results for Parallel-plate Channel

The effects of the Hartmann number,  $M$ , and Rayleigh number,  $Ra$ , on the dimensionless flow rate-pressure gradient ratio and Nusselt number are shown in Figures 2 and 3 for a fixed value of the wall conductance parameter,  $\phi_2 = 0.3$ , and no internal energy generation,  $F = 0$ .

Figure 2 shows that an increase in the Hartmann number (or equivalently, the magnetic field strength) decreases the flow rate at a fixed pressure gradient, regardless of free convection effects. However, as free convection increases ( $Ra$  increases), the

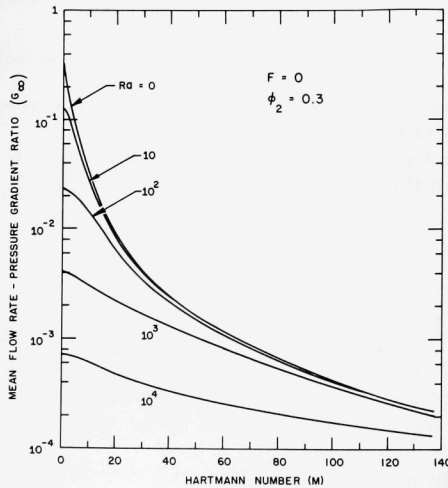


Fig. 2. Effect of the Hartmann and Rayleigh Numbers on  $G_{\infty}$  (Parallel-plate Channel)



effect of the Hartmann number on the flow rate decreases. Similarly, as the Hartmann number increases, the effect of free convection on the flow rate decreases.

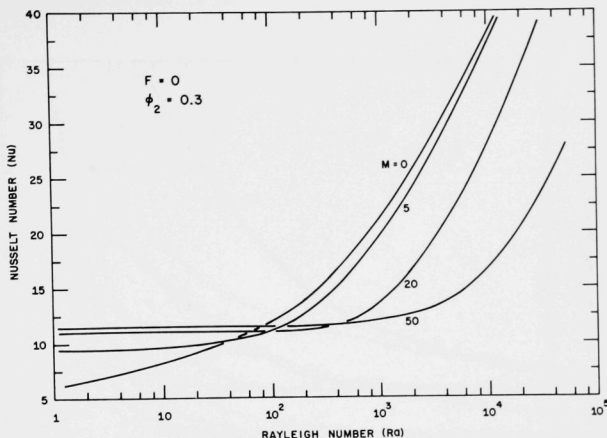


Fig. 3. Effect of the Hartmann and Rayleigh Numbers on the Nusselt Number (Parallel-plate Channel)

The Nusselt number is shown in Figure 3 as a function of Ra and M. It is evident that as the Hartmann number increases, larger and larger values of the Rayleigh number are required to increase the Nusselt number over its value at Ra = 0. Thus, the magnetic field seems to suppress the free-convection contribution to the heat transfer rate between the fluid and the channel walls.

This suppressing effect of the magnetic field is more clearly illustrated in Figure 4. Here, the ratio of the Nusselt number at an arbitrary value of the Rayleigh number to that at zero Rayleigh number is shown. When there is no magnetic field ( $M = 0$ ), a 29% increase in the last transfer rate is noted when Ra is only one. However, to achieve this increase when a magnetic field is present, larger and larger values of Ra are necessary as M is increased. For example, to increase  $Nu_{\infty}/Nu_{\infty}(Ra = 0)$  to 1.29, the following values of Ra are necessary: for  $M = 5$ ,  $Ra = 180$ ; for  $M = 20$ ,  $Ra = 1130$ ; and for  $M = 50$ ,  $Ra = 4800$ .

Therefore, if a criterion of a 10% increase in the Nusselt number is considered to be the point at which free-convection effects must be considered, a single plot may be obtained that shows the range of values of M and Ra for which free convection is important. This plot is shown in

Figure 5. Inspection of this figure indicates an approximately linear separation. The equation of the line for values of  $M \lesssim 8$  and  $Ra \gtrsim 100$  is approximately  $M = 5 + (Ra/40)$ .

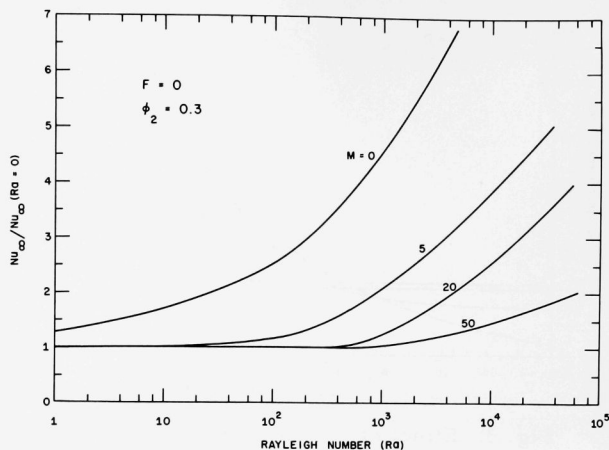


Fig. 4. Nusselt Number Ratio Variation with the Hartmann and Rayleigh Numbers (Parallel-plate Channel)

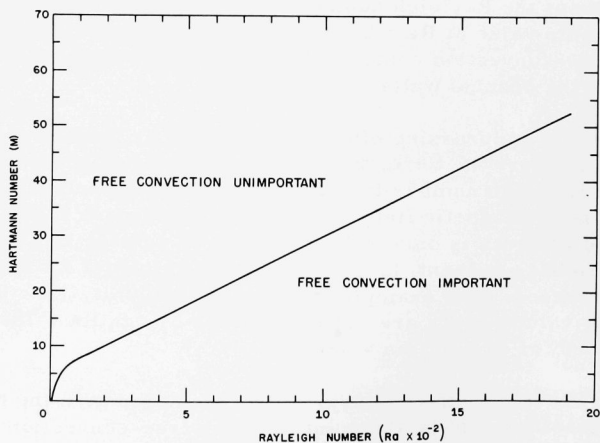


Fig. 5. Map of the  $M$ - $Ra$  Plane Showing Region of Free-convection Importance (Parallel-plate Channel)

The effect of the wall conductance parameter,  $\phi_2$ , upon the flow rate is shown in Figure 6, where  $\phi_2 = 0$  corresponds to the case of a nonelectrically-conducting wall, and  $\phi_2 = \infty$  corresponds to walls that are "perfect" electrical conductors.

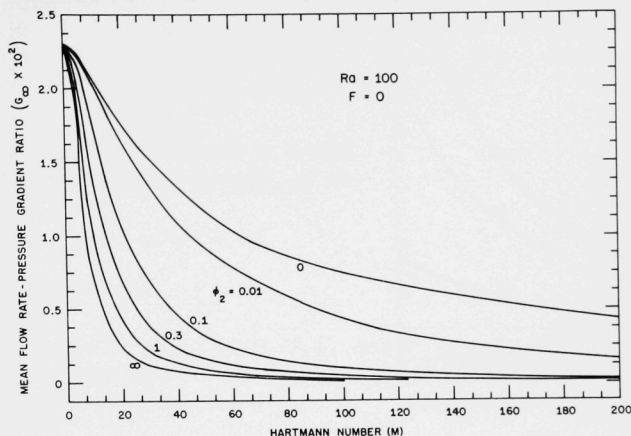


Fig. 6. Effect of the Wall Conductance Ratio and Hartmann Number on  $G_\infty$  (Parallel-plate Channel)

It is seen that  $\phi_2$  most strongly affects the flow rate for small values of  $M$ , and as  $M$  increases, the importance of  $\phi_2$  upon  $G_\infty$  decreases. The decrease in the flow rate with an increase in the wall conductance was explained physically in reference (7) for the case of zero free convection. That discussion still holds when free convection is important and thus is not repeated here.

An interesting result was observed when the effect of the wall conductance upon the Nusselt number was investigated. As  $\phi_2$  was varied between zero and infinity for fixed values of  $M$  and  $Ra$ , the Nusselt number remained unchanged to four decimal places. This was somewhat surprising due to the important effect of  $\phi_2$  on the flow rate. However, it appears that due to the definition of the Nusselt number used in this report, the combined effect of  $\phi_2$  on the flow rate and the bulk temperature difference exactly cancelled each other out.

Internal energy generation can also play a significant role, especially when free convection is possible. Figure 7 shows that the flow rate can be significantly increased as internal energy generation increases. However, for large values of  $M$ , the effect of  $F/G_\infty = Q/[Q + (2q_w/a)]$  is minor.

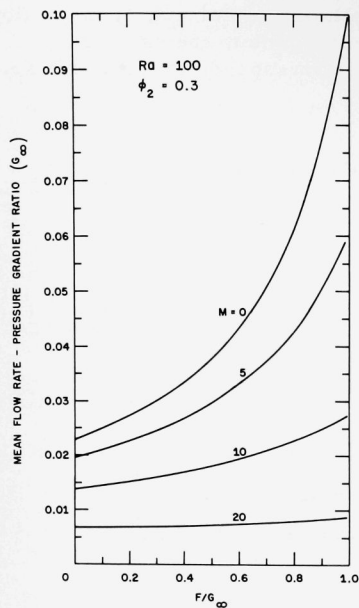


Fig. 7

Effect of Internal Energy Generation on  $G_\infty$  (Parallel-plate Channel)

The Nusselt number is shown in Figure 8 as a function of  $M$  and  $F/G_\infty$ . Again it is noted that internal energy generation is relatively unimportant when  $M$  is large, but must be considered when  $M$  is in the range of zero to about ten.

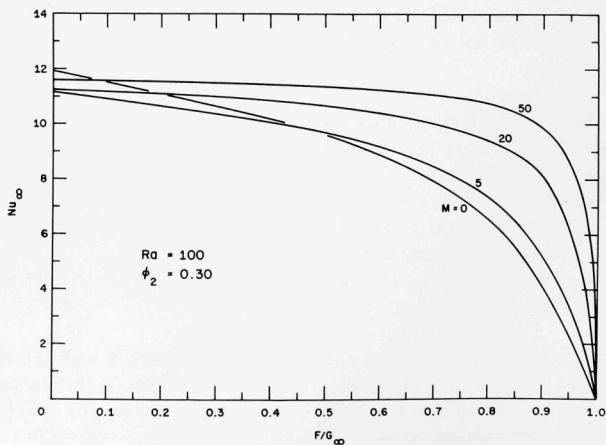


Fig. 8. Effect of Internal Energy Generation on the Nusselt Number (Parallel-plate Channel)

### C. Solution for Small Values of the Magnetic Prandtl Number

An alternative limiting solution of equations (16a), (22a), and (20a) can be obtained by restricting the analysis to vanishingly small values of the magnetic Prandtl number, i.e.,  $Pr_m \ll 1$ . If  $Pr_m$  approaches zero, a solution to equation (20a) that satisfies the boundary conditions (27) and (28) is just  $B = 0$ ; i.e., the induced magnetic field is negligibly small. Thus, from equation (14b),  $E_z = 0$ , so that, from (15a, b),  $E_y = \text{constant} = E_0$ . Thus, the ponderomotive force,  $\underline{J} \times \underline{B}$ , may be written as

$$\underline{J} \times \underline{B} = \sigma B_0 (E_0 - u B_0) \quad (54)$$

and equations (16a) and (22a) become

$$\nabla^2 U^* + Ra \theta^* - M^2 U^* = -1 \quad (55)$$

$$\nabla^2 \theta^* + F^* = U^* \quad (56)$$

where  $U^*$ ,  $\theta^*$ , and  $F^*$  differ from  $U$ ,  $\theta$ , and  $F$  by a constant factor, as shown in the Nomenclature. The boundary conditions on  $U^*$  and  $\theta^*$  are identical to those on  $U$  and  $\theta$ ; i.e.,

$$U^* = \theta^* = 0 \quad \text{at } \eta = \pm\gamma \quad \text{and at } \zeta = \pm 1. \quad (58a, b)$$

The special case of zero free-convection ( $Ra = 0$ ) has been solved by Ryabinin and Khozhainov,<sup>(23)</sup> and of nonmagnetic flow ( $M = 0$ ) by Han.<sup>(24)</sup> These solutions may be obtained from the more general form derived in the succeeding paragraphs by substituting the appropriate value of  $Ra$  or  $M$ .

Equations (55) and (56) can be solved by means of finite Fourier transforms (for a thorough treatment of these transforms, the interested reader is referred to the text by Churchill).<sup>(25)</sup> Since this method of solution is fairly routine and straightforward, only the final results for  $U^*$  and  $\theta^*$  will be presented:

$$U^*(\eta, \zeta) = \frac{16}{\pi^2} \sum_{\text{odd } m, n} \frac{A_{mn}}{mn} \left[ 1 + \frac{Ra F^*}{(n\pi)^2 + (m\pi/\gamma)^2} \right] \sin \left[ \frac{n\pi(\zeta + 1)}{2} \right] \sin \left[ \frac{m\pi(\eta + \gamma)}{2\gamma} \right], \quad (59)$$

and

$$\theta^*(\eta, \zeta) = \frac{16}{\pi^2} \sum_{\text{odd } m, n} \left\{ \frac{F^* - A_{mn} \left[ 1 + \frac{Ra F^*}{(n\pi)^2 + (m\pi/\gamma)^2} \right]}{[mn(n\pi)^2 + (m\pi/\gamma)^2]} \right\} \sin \left[ \frac{n\pi(\zeta + 1)}{2} \right] \sin \left[ \frac{m\pi(\eta + \gamma)}{2\gamma} \right], \quad (60)$$

where

$$A_{mn}^{-1} = (n\pi)^2 + (m\pi/\gamma)^2 + M^2 + \frac{Ra}{(n\pi)^2 + (m\pi/\gamma)^2} \quad (61)$$

### 1. Relationship of Pressure Drop to Flow Rate

The following relationship between the pressure drop and the mass average velocity (or flow rate) can be obtained from the expression for  $U^*(\eta, \xi)$  in equation (59) and the definition of  $\bar{u}$  from equation (41):

$$\frac{\bar{u}}{a^2 \left( -\frac{\partial p}{\partial x} \right) - \rho g + \gamma B_0 E_0} = G^* = \frac{1}{4\gamma} \int_{-1}^{+1} \int_{-\gamma}^{+\gamma} U^*(\eta, \xi) d\eta d\xi. \quad (62)$$

Performing the integration in (62), using the expression for  $U^*(\eta, \xi)$  from (59), results in

$$G^* = \frac{64}{\pi^4} \sum_{\text{odd } m, n} \frac{A_{mn}}{m^2 n^2} \left\{ \left[ 1 + \frac{Ra F^*}{(n\pi)^2 + (m\pi/\gamma)^2} \right] \right\}. \quad (63)$$

### 2. Heat Transfer

As in the previous section, the heat transfer results may be conveniently presented in terms of the temperature difference between the wall and the "bulk" fluid. A straightforward derivation, utilizing the definitions of  $U^*$ ,  $\theta^*$ ,  $\eta$ ,  $\xi$ , and  $T_B$ , results in

$$Nu^* = \left( \frac{F^* - G^*}{1 + 1/\gamma} \right) \left( \frac{1}{4\gamma G^*} \int_{-1}^{+1} \int_{-\gamma}^{+\gamma} U^*(\eta, \xi) \theta^*(\eta, \xi) d\eta d\xi \right)^{-1}, \quad (64)$$

where

$$Nu^* = [(q_w \cdot 2a)/k(T_w - T_B)].$$

Utilizing the expressions for  $\theta^*(\eta, \xi)$  and  $U^*(\eta, \xi)$  from equations (59) and (60), the integral in equation (64) can be evaluated to yield

$$\frac{G^*(G^* - F^*)}{Nu^*(1 + 1/\gamma)} = \frac{64}{\pi^4} \sum_{\text{odd } m, n} \frac{A_{mn}}{m^2 n^2} \left[ 1 + \frac{Ra F^*}{(n\pi)^2 + (m\pi/\gamma)^2} \right] \left\{ \frac{-F^* + A_{mn} \left[ 1 + \frac{Ra F^*}{(n\pi)^2 + (m\pi/\gamma)^2} \right]}{(n\pi)^2 + (m\pi/\gamma)^2} \right\} \quad (65)$$

### 3. Discussion of Results for Rectangular Channels

The velocity and temperature profiles as calculated from equations (59) and (60) are shown in Figures 9 and 10 respectively. For ease in presentation, the values were calculated along the channel diagonal  $\xi = \eta/\gamma$ . As is to be expected, increasing the Hartmann number decreases both the local velocity and the difference between the local fluid temperature and the wall temperature.

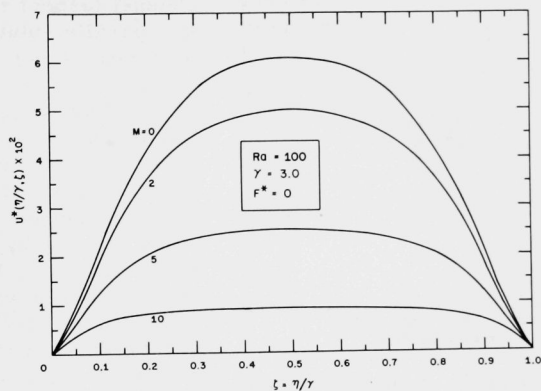


Fig. 9. Velocity Profile Variation with the Hartmann Number (Small  $Pr_m$  Case)

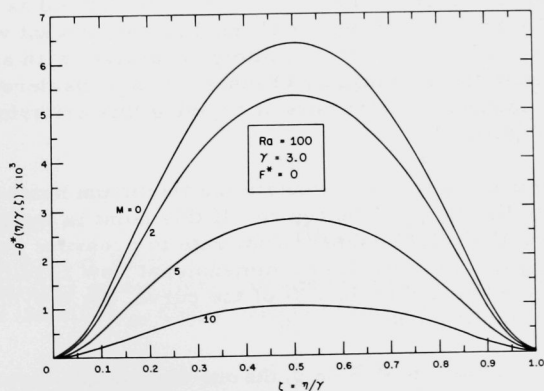


Fig. 10. Temperature Profile Variation with the Hartmann Number (Small  $Pr_m$  Case)



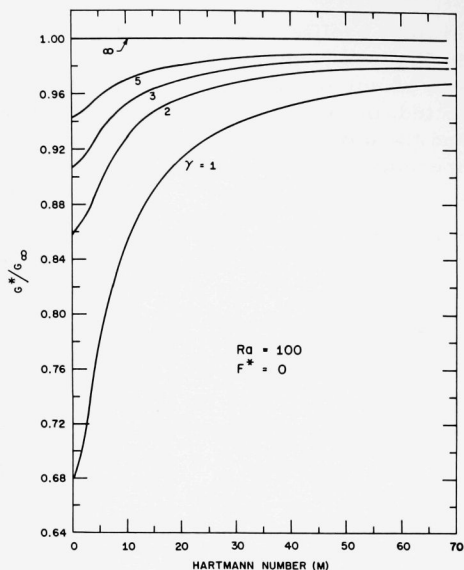


Fig. 11. Effect of the Aspect Ratio and Hartmann Number on a Flow Rate Ratio (Small  $Pr_m$  Case)

The dependence of the flow rate upon the aspect ratio,  $\gamma$ , and the Hartmann number is shown in Figure 11. To illustrate the effects of aspect ratio on the flow velocity, the graph is presented in terms of  $G^*/G_\infty$  or, equivalently, the ratio of the mean velocity in a rectangular channel (aspect ratio =  $\gamma$ ) to that in a parallel-plate channel (aspect ratio =  $\infty$ ).

For small values of the Hartmann number, varying the aspect ratio from infinity (parallel-plate channel) to one (square channel) reduces the mean velocity by about 30%. However, as the Hartmann number increases, the effect of  $\gamma$  decreases markedly. Figure 11 shows further that a criterion can be established that can be used to determine when a particular rectangular channel can be considered to be a parallel-plate channel when

a magnetic field is present. Let the criterion be defined as follows: if the mean flow velocity in a rectangular channel is 95% of what would be obtained if the two side walls were infinitely separated, with all other conditions unchanged, the rectangular channel can be considered to be a parallel-plate channel. The results of applying this criterion to Figure 11 are shown in Figure 12.

To use Figure 12, calculate the Hartmann number and the aspect ratio and locate the point on the figure. If this point is to the right and above the curve, the relationship of flow rate to pressure gradient can be calculated using the simplified, one-dimensional flow results. However, if the point lies below and to the left of the curve, the two-dimensional flow equation must be used.

For values of  $M \gtrsim 38.5$ , the one-dimensional approximation can always be used independent of the aspect ratio (for values of  $Ra \lesssim 100$  and no internal energy generation). Liquid metal MHD power generators normally operate at values of  $M$  greater than 100.

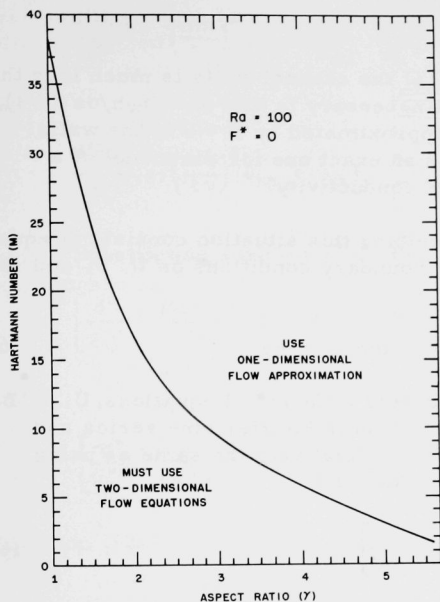


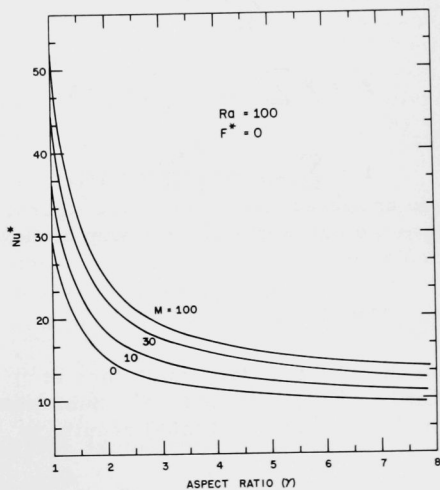
Fig. 12

Map of  $M$ - $\gamma$  Plane Showing  
Region of Two-dimensional  
Effects (Small  $Pr_m$  Case)

Finally, the Nusselt number as a function of the Hartmann number and aspect ratio is shown in Figure 13. The Nusselt number decreases with an increase in the aspect ratio and a decrease in the Hartmann number.

Fig. 13

Effect of the Aspect Ratio and  
Hartmann Number on the Nus-  
selt Number (Small  $Pr_m$  Case)



#### D. Nonconducting Channel Walls

If the electrical conductivity of the channel walls is much less than that of the fluid (actually, all that is necessary is that  $\phi = \sigma_w h / \sigma a \ll 1$ ), the boundary condition (26) can be approximated by  $B = 0$  at the walls. Thus, the solution to be presented is an exact one for the model of a channel with walls of zero electrical conductivity.

The differential system describing this situation consists of equations (16a), (22a), and (20a), and the boundary conditions on  $U$ ,  $\theta$ , and  $B$  are

$$U = \theta = B = 0 \quad \text{at } \eta = \pm\gamma \quad \text{and } \zeta = \pm\gamma. \quad (66)$$

To reduce this system to ordinary differential equations,  $U$ ,  $\theta$ ,  $B$ ,  $F$ , and  $l$  will be expressed in terms of their Fourier sine series and substituted into the governing relations (effectively the same as using finite Fourier sine transforms).<sup>(26)</sup> Thus, let

$$B(\eta, \zeta) = \sum_m B_m(\zeta) \sin \left[ \frac{m\pi}{2} (\eta + \gamma) \right], \quad (67)$$

$$U(\eta, \zeta) = \sum_m U_m(\zeta) \sin \left[ \frac{m\pi}{2} (\eta + \gamma) \right], \quad (68)$$

$$\theta(\eta, \zeta) = \sum_m \theta_m(\zeta) \sin \left[ \frac{m\pi}{2\gamma} (\eta + \gamma) \right], \quad (69)$$

$$F = F \sum a_m \sin \left[ \frac{m\pi}{2\gamma} (\eta + \gamma) \right], \quad (70)$$

$$l = \sum a_m \sin \left[ \frac{m\pi}{2\gamma} (\eta + \gamma) \right], \quad (71)$$

and

$$a_m = \frac{2}{\pi} \left( \frac{1 - \cos m\pi}{m} \right). \quad (71a)$$

Note that the boundary conditions at  $\eta = \pm\gamma$  are identically satisfied by equations (67), (68), and (69). Substituting these series forms into equations (16a), (22a), and (20a) results in

$$\frac{d^2 B_m}{d\zeta^2} - \left( \frac{m\pi}{2\gamma} \right)^2 B_m + R_m \frac{dU_m}{d\zeta} = 0, \quad (72)$$

$$\frac{d^2 U_m}{d\xi^2} - \left(\frac{m\pi}{2\gamma}\right)^2 U_m + \frac{M^2}{R_m} \frac{dB_m}{d\xi} + Ra\theta_m = -a_m, \quad (73)$$

and

$$\frac{d^2 \theta_m}{d\xi^2} - \left(\frac{m\pi}{2\gamma}\right)^2 \theta_m + a_m F = U_m. \quad (74)$$

Substituting equation (74) into equations (72) and (73) results in

$$\left[ \frac{d^2}{d\xi^2} - \left(\frac{m\pi}{2\gamma}\right)^2 \right] \left( B_m + R_m \frac{d\theta_m}{d\xi} \right) = 0, \quad (72a)$$

and

$$\left[ \frac{d^2}{d\xi^2} - \left(\frac{m\pi}{2\gamma}\right)^2 \right]^2 \theta_m + Ra\theta_m + \frac{M^2}{R_m} \frac{dB_m}{d\xi} = -a_m \left[ 1 - \left(\frac{m\pi}{2\gamma}\right)^2 F \right] \quad (73a)$$

Equation (72a) implies that

$$B_m + R_m \frac{d\theta_m}{d\xi} = \phi_m(\xi), \quad (75)$$

where

$$\frac{d^2 \phi_m}{d\xi^2} - \left(\frac{m\pi}{2\gamma}\right)^2 \phi_m = 0. \quad (75a)$$

Thus,  $\phi_m(\xi)$  is just

$$\phi_m(\xi) = p e^{\left(\frac{m\pi}{2\gamma}\right)\xi} + q e^{-\left(\frac{m\pi}{2\gamma}\right)\xi}, \quad (75b)$$

where  $p$  and  $q$  must be determined from the boundary conditions on  $B_m$  and  $\theta_m$  applied to equation (74). Substituting (74) into (73a) finally results in the following equation for  $\theta_m$ :

$$\frac{d^4 \theta_m}{d\xi^4} - \left[ M^2 + 2\left(\frac{m\pi}{2\gamma}\right)^2 \right] \frac{d^2 \theta_m}{d\xi^2} + \left[ Ra + \left(\frac{m\pi}{2\gamma}\right)^4 \right] \theta_m = -\frac{M^2}{R_m} \frac{d\phi_m}{d\xi} - a_m \left[ 1 - \left(\frac{m\pi}{2\gamma}\right)^2 F \right] \quad (76)$$

From equations (66), (68), (69), and (74), the boundary conditions on  $\theta_m(\xi)$  can be shown to be

$$\frac{d^2\theta_m}{d\xi^2} + a_m F = \theta_m = 0 \quad \text{at } \xi = \pm 1. \quad (77a,b)$$

An examination of indicial equation corresponding to equation (75) shows that the functional form of  $\theta_m(\xi)$  depends upon the relative magnitudes of the terms  $(m\pi/2\gamma)^2$  and  $(M^2/4)(4Ra/M^4 - 1)$ . Thus, solutions of equation (76) can be obtained and are presented in Appendix C.

When the expressions for  $\theta_m(\xi)$  from Appendix C are used, the dimensionless velocity function,  $U_m(\xi)$ , and the dimensionless magnetic field function,  $B_m(\xi)$ , can be directly calculated from equations (74) and (75), respectively. These results are also shown in Appendix C.

When the expressions for  $\theta_{mi}$ ,  $U_{mi}$ , and  $B_{mi}$ ,  $i = 1, 3$ , from Appendix C are used, the actual temperature, velocity, and magnetic field functions can be constructed from equations (67), (68), and (69). Thus,

$$B(\eta, \xi) = \sum_{m=1}^{m_0} B_{m1}(\xi) \sin \left[ \frac{m\pi}{2\gamma} (\eta + \gamma) \right] + B_2(\xi) \sin \left[ \frac{M}{2} \left( \frac{4Ra}{M^4} - 1 \right)^{1/2} (\eta + \gamma) \right] \\ + \sum_{m>m_0}^{\infty} B_{m3}(\xi) \sin \left[ \frac{m\pi}{2\gamma} (\eta + \gamma) \right], \quad (88)$$

$$U(\eta, \xi) = \sum_{m=1}^{m_0} U_{m1}(\xi) \sin \left[ \frac{m\pi}{2\gamma} (\eta + \gamma) \right] + U_2(\xi) \sin \left[ \frac{M}{2} \left( \frac{4Ra}{M^4} - 1 \right)^{1/2} (\eta + \gamma) \right] \\ + \sum_{m>m_0}^{\infty} U_{m3}(\xi) \sin \left[ \frac{m\pi}{2\gamma} (\eta + \gamma) \right], \quad (89)$$

and

$$\theta(\eta, \xi) = \sum_{m=1}^{m_0} \theta_{m1}(\xi) \sin \left[ \frac{m\pi}{2\gamma} (\eta + \gamma) \right] + \theta_2(\xi) \sin \left[ \frac{M}{2} \left( \frac{4Ra}{M^4} - 1 \right)^{1/2} (\eta + \gamma) \right] \\ + \sum_{m>m_0}^{\infty} \theta_{m3}(\xi) \sin \left[ \frac{m\pi}{2\gamma} (\eta + \gamma) \right], \quad (90)$$

where

$$m_0 = (M/\pi) [(4Ra/M^4) - 1]^{1/2}. \quad (90a)$$

### 1. Pressure Drop Parameter

From the definition of  $\bar{u}$ , it may be shown that

$$G = \frac{1}{4\gamma(1+1/\gamma)} \int_{-1}^{+1} \int_{-\gamma}^{+\gamma} U(\eta, \xi) d\eta d\xi. \quad (91)$$

### 2. Heat Transfer Results

Defining a Nusselt number as in the previous sections, i.e.,

$$Nu \equiv \left[ \frac{q_w \cdot 2a}{k(T_w - T_B)} \right], \quad (93)$$

one obtains the relation

$$Nu = \frac{4\gamma G(G - F)}{(1 + 1/\gamma)} \left( \int_{-1}^{+1} \int_{-\gamma}^{+\gamma} U \theta d\eta d\xi \right)^{-1}. \quad (94)$$

Utilizing the solutions obtained for  $U$  and  $\theta$  in equations (89) and (90), and carrying out the indicated operations, one obtains

$$\begin{aligned} \frac{4G(G - F)}{Nu(1 + 1/\gamma)} = & - \sum_{m=1}^{m \leq m_0} \int_{-1}^{+1} U_{m1}(\xi) \theta_{m1}(\xi) d\xi - \int_{-1}^{+1} U_2(\xi) \theta_2(\xi) d\xi \\ & - \sum_{m > m_0}^{\infty} \int_{-1}^{+1} U_{m3}(\xi) \theta_{m3}(\xi) d\xi. \end{aligned} \quad (95)$$

Using the expressions for  $U_{mi}$  and  $\theta_{mi}$  from equations (78) through (86), the integrations can be carried out, and the results are shown in Appendix C.

### 3. Results and Discussion

Due to the extreme complexity of the results presented in this section and their limited application, no numerical results are presented.

## IV. CONCLUSIONS

In this report, the steady, combined, free and forced convective flow of an electrically-conducting fluid through a vertical channel in the presence of a horizontal magnetic field has been studied. Three distinct physical

situations have been investigated: (a) parallel-plate channel with walls of arbitrary electrical conductivity, (b) rectangular channel containing a fluid with a very small magnetic Prandtl number, and (c) rectangular channel with nonconducting walls. Numerical results were presented for only the first two cases.

In addition to obtaining some basic information on the interaction of mechanical, thermal, and electromagnetic forces, several practical results were noted. It was found that a magnetic field strongly inhibits free convection, and a criterion was established that indicates when free convection may or may not be neglected, based on the relative values of the Rayleigh and Hartmann numbers. This criterion may be stated as follows. If  $M > 5 + (Ra/40)$ , the contribution of free convection to the total heat transfer rate between the fluid and the wall is less than 10% and can be neglected. If  $M < 5 + (Ra/40)$ , the contribution is greater than 10% and should be considered.

It was also noted that a magnetic field sufficiently flattens the velocity profile in a channel so that the flow can be considered one-dimensional in many cases. A relationship between the Hartmann number,  $M$ , and the aspect ratio,  $\gamma$ , presented in Figure 12, shows when the one-dimensional approximation can be made allowing a 5% error in calculating the ratio of the flow rate to the pressure gradient. It was shown that when free convection effects are not important and  $M \gtrsim 38.5$ , all rectangular channels may be considered to be parallel-plate channels for the purpose of computing the ratio of the flow rate to the pressure gradient.

The work presented in this report is a continuation of that presented in ANL-6937, which considered the unsteady, convective, magnetohydrodynamic flow in a parallel-plate channel.

## APPENDIX A

Fully-developed Assumption

The restrictions that are placed upon the pressure and temperature because of the fully-developed flow and heat transfer assumption are derived in this Appendix.

From equations (17) and (14a), it is deduced that

$$-\frac{\partial p}{\partial y} - \frac{1}{2\mu_0} \frac{\partial}{\partial y} (B_x^2) = 0, \quad (A1)$$

so that

$$p(x, y, z) = p_1(x, z) - \frac{1}{2\mu_0} B_x^2(y, z), \quad (A2)$$

and

$$\frac{\partial}{\partial x} [p(x, y, z)] = \frac{\partial}{\partial x} [p_1(x, z)]. \quad (A2a)$$

But from equations (18) and (13a),

$$-\frac{\partial p}{\partial z} - \frac{1}{2\mu_0} \frac{\partial}{\partial z} (B_x^2) = 0, \quad (A3)$$

so that

$$\frac{\partial^2 p}{\partial x \partial z} = 0. \quad (A4)$$

Therefore, since  $p(x, y, z)$  is continuous and all of its partial derivatives exist, the order of differentiation is immaterial, and a comparison of (A2a) and (A4) shows that

$$\frac{\partial}{\partial x} [p(x, y, z)] = \text{function of } x \text{ only.} \quad (A4a)$$

Combining equations (16), (13a), and (24) results in

$$\rho \nu \left( \frac{\partial^2 u}{\partial z^2} + \frac{\partial^2 u}{\partial y^2} \right) - \rho_w g + \frac{B_0}{\mu_0} \frac{\partial B_x}{\partial z} + \rho_w \beta g (T - T_w) = \frac{\partial p}{\partial x}. \quad (A5)$$

Differentiating both sides of this equation with respect to  $x$  gives



$$\rho_w \beta g \frac{\partial}{\partial x} (T - T_w) = \frac{\partial^2 p}{\partial x^2}. \quad (A6)$$

But,  $\partial^2 p / \partial x^2$  can be only a function of  $x$ , so this implies that

$$T - T_w = T_1(x) + T_2(y, z). \quad (A7)$$

Substituting this result into equation (19) with rearrangement shows that

$$\rho c u \left( \frac{dT_w}{dx} + \frac{dT_1}{dx} \right) - k \left( \frac{d^2 T_w}{dx^2} + \frac{d^2 T_1}{dx^2} \right) = k \left( \frac{\partial^2 T_2}{\partial y^2} + \frac{\partial^2 T_2}{\partial z^2} \right) + Q. \quad (A8)$$

Now, it is apparent that the right side of equation (A8) is a function of  $y$  and  $z$  only, while the left side is a function of  $y$ ,  $z$ , and  $x$ . The only  $x$ -dependence arises from the terms involving  $T_w$  and  $T_1$ , and the previous statement can be self-consistent only when

$$\frac{dT_w}{dx} + \frac{dT_1}{dx} = \text{constant}. \quad (A9)$$

Thus,

$$T_w(x) + T_1(x) = Ax. \quad (A10)$$

This results in

$$T(x, y, z) = Ax + T_2(y, z). \quad (A11)$$

But,

$$T_w(x) = T(x, y_w, z_w),$$

where  $y_w$  and  $z_w$  are the values of  $y$  and  $z$  at the wall. Thus,

$$T_w(x) = Ax + T_2(y_w, z_w),$$

and

$$T(x, y, z) - T_w(x) = T_2(y, z) - T_2(y_w, z_w). \quad (A12)$$

It is now seen that  $T - T_w$  is independent of  $x$ . By inspection of equations (A12) and (A6), it is apparent that  $\partial^2 p / \partial x^2 = 0$ , and remembering the result in equation (A4a),

$$\frac{\partial p}{\partial x} = \text{constant}, \quad (\text{A13})$$

or,

$$p(x, y, z) = p_2(y, z) + \kappa' x, \quad (\text{A14})$$

where  $\kappa'$  is a constant.

APPENDIX B  
Parallel-plate Case Results

1. Detailed Solutions

a.  $M^4 > 4Ra > 0$ :

$$U_{\infty} = F - A_1 \cosh \lambda_1 \zeta + A_2 \cosh \lambda_2 \zeta \quad (B1)$$

$$\begin{aligned} -Ra\theta_{\infty} = & \left[ 1 + (\kappa_1 M^2 Pr_m / Pr) - M^2 F \right] - A_1 (\lambda_1^2 - M^2) \cosh \lambda_1 \zeta \\ & + A_2 (\lambda_2^2 - M^2) \cosh \lambda_2 \zeta \end{aligned} \quad (B2)$$

$$\begin{aligned} B_{\infty} = & \kappa_1 (\zeta + 1 + \phi_2) - (Pr / Pr_m) \left[ F(\zeta + 1) - (A_1 / \lambda_1) (\sinh \lambda_1 \zeta + \sinh \lambda_1) \right. \\ & \left. + (A_2 / \lambda_2) (\sinh \lambda_2 \zeta + \sinh \lambda_2) \right] \end{aligned} \quad (B3)$$

b.  $M^4 = 4Ra > 0$ :

$$U_{\infty} = F + A_3 \zeta \sinh \lambda \zeta + A_4 \cosh \lambda \zeta \quad (B4)$$

$$\begin{aligned} -Ra\theta_{\infty} = & \left[ 1 + (\kappa_2 M^2 Pr_m / Pr) - M^2 F \right] + \left[ A_4 (\lambda^2 - M^2) + 2\lambda A_3 \right] \cosh \lambda \zeta \\ & + A_3 (\lambda^2 - M^2) \zeta \sinh \lambda \zeta \end{aligned} \quad (B5)$$

$$\begin{aligned} B_{\infty} = & \kappa_2 (\zeta + 1 + \phi_2) - (Pr_m / Pr) \left[ F(\zeta + 1) + (A_4 / \lambda) (\sinh \lambda \zeta + \sinh \lambda) \right. \\ & \left. + (A_3 / \lambda^2) (\lambda \zeta \cosh \lambda \zeta - \sinh \lambda \zeta + \lambda \cosh \lambda - \sinh \lambda) \right] \end{aligned} \quad (B6)$$

c.  $M^4 < 4Ra$ :

$$U_{\infty} = F + A_5 \cos \lambda_3 \zeta \cosh \lambda_4 \zeta + A_6 \sin \lambda_3 \zeta \sinh \lambda_4 \zeta \quad (B7)$$

$$\begin{aligned} -Ra\theta_{\infty} = & 1 + (\kappa_3 M^2 Pr_m / Pr) - M^2 F + \left[ A_5 (\lambda_4^2 - \lambda_3^2 - M^2) + 2\lambda_3 \lambda_4 A_6 \right] \cos \lambda_3 \zeta \cosh \lambda_4 \zeta \\ & + \left[ A_6 (\lambda_4^2 - \lambda_3^2 - M^2) - 2\lambda_3 \lambda_4 A_5 \right] \sin \lambda_3 \zeta \sinh \lambda_4 \zeta \end{aligned} \quad (B8)$$

$$\begin{aligned} B_{\infty} = & \kappa_3 (\zeta + 1 + \phi_2) - (Pr_m / Pr) \left[ F(\zeta + 1) \right. \\ & + \left( \frac{\lambda_3 A_5 + \lambda_4 A_6}{\lambda_3^2 + \lambda_4^2} \right) (\sin \lambda_3 \zeta \cosh \lambda_4 \zeta + \sin \lambda_3 \cosh \lambda_4) \\ & \left. + \left( \frac{\lambda_4 A_5 - \lambda_3 A_6}{\lambda_3^2 + \lambda_4^2} \right) (\cos \lambda_3 \zeta \sinh \lambda_4 \zeta + \cos \lambda_3 \sinh \lambda_4) \right] \end{aligned} \quad (B9)$$

d.  $Ra < 0$  (for all  $M$ ):

$$U_{\infty} = F - A_7 \cosh \lambda_6 \zeta + A_8 \cos \lambda_5 \zeta \quad (B10)$$

$$\begin{aligned} -Ra\theta_{\infty} &= 1 + (\kappa_4 M^2 Pr_m / Pr) - M^2 F + A_7 (M^2 - \lambda_6^2) \cosh \lambda_6 \zeta \\ &\quad - A_8 (M^2 + \lambda_5^2) \cos \lambda_5 \zeta \end{aligned} \quad (B11)$$

$$\begin{aligned} B_{\infty} &= \kappa_4 (\zeta + 1 + \phi_2) - (Pr_m / Pr) \left[ F(\zeta + 1) - (A_7 / \lambda_6) (\sinh \lambda_6 \zeta + \sinh \lambda_6) \right. \\ &\quad \left. + (A_8 / \lambda_5) (\sin \lambda_5 \zeta + \sin \lambda_5) \right] \end{aligned} \quad (B12)$$

## 2. Relationship of Pressure Gradient to Flow Rate

a.  $M^4 > 4Ra > 0$ :

$$G_{\infty} = F - (A_1 / \lambda_1) \sinh \lambda_1 + (A_2 / \lambda_2) \sinh \lambda_2 \quad (B13)$$

b.  $M^4 = 4Ra > 0$ :

$$G_{\infty} = F + \left[ (A_3 + A_4) / \lambda \right] \sinh \lambda - (A_3 / \lambda^2) \cosh \lambda \quad (B14)$$

c.  $M^4 < 4Ra$ :

$$G_{\infty} = F + \left( \frac{\lambda_3 A_5 + \lambda_4 A_6}{\lambda_3^2 + \lambda_4^2} \right) \sin \lambda_3 \cosh \lambda_4 + \left( \frac{\lambda_4 A_5 - \lambda_3 A_6}{\lambda_3^2 + \lambda_4^2} \right) \cos \lambda_3 \sinh \lambda_4 \quad (B15)$$

d.  $Ra < 0$  (for all  $M$ ):

$$G_{\infty} = F - (A_7 / \lambda_6) \sinh \lambda_6 + (A_8 / \lambda_5) \sin \lambda_5 \quad (B16)$$

## 3. Nusselt Numbers

a.  $M^4 > 4Ra > 0$ :

$$\begin{aligned} 2G_{\infty}(G_{\infty} - F) / Nu_{\infty} &= \frac{F}{2Ra} \left[ 1 + (\kappa_1 M^2 / Rm) - M^2 F \right] - \left( \frac{A_1 \sinh \lambda_1}{2\lambda_1 Ra} \right) \left[ 1 + (\kappa_1 M^2 / Rm) + F(\lambda_1^2 - 2M^2) \right] \\ &\quad + \left( \frac{A_2 \sinh \lambda_2}{2\lambda_2 Ra} \right) \left[ 1 + (\kappa_1 M^2 / Rm) + F(\lambda_2^2 - 2M^2) \right] \\ &\quad + \frac{A_1^2 (\lambda_1^2 - M^2)}{4Ra} \left( 1 + \frac{\sinh 2\lambda_1}{2\lambda_1} \right) + \frac{A_2^2 (\lambda_2^2 - M^2)}{4Ra} \left( 1 + \frac{\sinh 2\lambda_2}{2\lambda_2} \right) \\ &\quad - \frac{A_1 A_2 (\lambda_1^2 + \lambda_2^2 - 2M^2)}{2Ra (\lambda_1^2 - \lambda_2^2)} (\lambda_1 \sinh \lambda_1 \cosh \lambda_2 - \lambda_2 \sinh \lambda_2 \cosh \lambda_1) \end{aligned} \quad (B17)$$

b.  $M^4 = 4Ra > 0$ :

$$\begin{aligned}
 \frac{2G_{\infty}(G_{\infty} - F)}{Nu_{\infty}} &= \frac{F}{2Ra} \left[ 1 + (\kappa_2 M^2 / Rm) - M^2 F \right] + \frac{A_3}{2\lambda^2 Ra} \left[ 1 + (\kappa_2 M^2 / Rm) + F(\lambda^2 - 2M^2) \right] (\lambda \cosh \lambda - \sinh \lambda) \\
 &+ \frac{A_3^2(\lambda^2 - M^2)}{4Ra} \left[ \left( 1 + \frac{1}{2\lambda^2} \right) \frac{\sinh 2\lambda}{2\lambda} - \frac{1}{3} - \frac{\cosh 2\lambda}{2\lambda^2} \right] \\
 &+ \frac{A_3}{8\lambda^2 Ra} \left[ \lambda A_3 + A_4(\lambda^2 - M^2) \right] (2\lambda \cosh 2\lambda - \sinh 2\lambda) \\
 &+ \left( \frac{\sinh \lambda}{2\lambda Ra} \right) \left[ A_4 \left( 1 + (\kappa_2 M^2 / Rm) \right) + FA_4(\lambda^2 - 2M^2) + 2\lambda A_3 F \right] \\
 &+ \frac{A_4}{4Ra} \left( 1 + \frac{\sinh 2\lambda}{2\lambda} \right) \left[ 2\lambda A_3 + A_4(\lambda^2 - M^2) \right] \quad (B18)
 \end{aligned}$$

c.  $M^4 < 4Ra$ :

$$\begin{aligned}
 2G_{\infty}(G_{\infty} - F)/Nu_{\infty} &= \frac{F}{2Ra} \left[ 1 + (\kappa_3 M^2 / Rm) - M^2 F \right] + \left[ \frac{1}{2Ra(\lambda_3^2 + \lambda_4^2)} \right] \left\{ \left[ 1 + (\kappa_3 M^2 / Rm) \right. \right. \\
 &+ \left. \left. F(\lambda_4^2 - \lambda_3^2 - 2M^2) \right] \left[ (\lambda_3 A_5 + \lambda_4 A_6) \sin \lambda_3 \cosh \lambda_4 \right. \right. \\
 &+ \left. \left. (\lambda_4 A_5 - \lambda_3 A_6) \cos \lambda_3 \sinh \lambda_4 \right] + 2F\lambda_3 \lambda_4 \left[ (\lambda_3 A_6 - \lambda_4 A_5) \sin \lambda_3 \cosh \lambda_4 \right. \right. \\
 &+ \left. \left. (\lambda_4 A_6 + \lambda_3 A_5) \cos \lambda_3 \sinh \lambda_4 \right] \right\} + \left( \frac{A_5^2 + A_6^2}{8Ra} \right) (\lambda_4^2 - \lambda_3^2 - M^2) \\
 &\left[ 1 + \frac{\sinh 2\lambda_4}{2\lambda_4} + \frac{\sin 2\lambda_3}{2\lambda_3} + \frac{1}{2} (\lambda_3 \sin 2\lambda_3 \cosh 2\lambda_4 - \lambda_4 \cos 2\lambda_3 \sinh 2\lambda_4) \right] \\
 &+ \frac{\lambda_3 \lambda_4 A_5 A_6}{2Ra} + \left[ \frac{\lambda_4 \sin 2\lambda_3 \cosh 2\lambda_4 - \lambda_3 \cos 2\lambda_3 \sinh 2\lambda_4}{8Ra(\lambda_3^2 + \lambda_4^2)} \right] \\
 &\left[ \lambda_3 \lambda_4 (A_6^2 - A_5^2) + A_5 A_6 (\lambda_4^2 - \lambda_3^2 - M^2) \right] \quad (B19)
 \end{aligned}$$

d.  $Ra < 0$  (for all  $M$ ):

$$\begin{aligned}
 2G_{\infty}(G_{\infty} - F)/Nu_{\infty} &= \frac{F}{2Ra} \left[ 1 + (\kappa_4 M^2 / Rm) - M^2 F \right] - \left( \frac{A_7 \sinh \lambda_6}{2Ra\lambda_6} \right) \left[ 1 + (\kappa_4 M^2 / Rm) + F(\lambda_6^2 - 2M^2) \right] \\
 &+ \left( \frac{A_8 \sin \lambda_5}{2\lambda_5 Ra} \right) \left[ 1 + (\kappa_4 M^2 / Rm) - F(\lambda_5^2 + 2M^2) \right] + \frac{A_7^2(\lambda_6^2 - M^2)}{4Ra} \left( 1 + \frac{\sinh 2\lambda_6}{2\lambda_6} \right) \\
 &- \frac{A_8^2(\lambda_5^2 + M^2)}{4Ra} \left( 1 + \frac{\sin \lambda_5}{2\lambda_5} \right) + \frac{A_7 A_8 (\lambda_5^2 - \lambda_6^2 + 2M^2)}{2Ra(\lambda_5^2 + \lambda_6^2)} (\lambda_5 \sin \lambda_5 \cosh \lambda_6 + \lambda_6 \cos \lambda_5 \sinh \lambda_6) \quad (B20)
 \end{aligned}$$

#### 4. Integration Constants

$$A_1 = \frac{1}{\cosh \lambda_1} \left[ \frac{1 + (\kappa_1 M^2 / Rm) - \lambda_2^2 F}{\lambda_1^2 - \lambda_2^2} \right]$$

$$A_2 = \frac{1}{\cosh \lambda_2} \left[ \frac{1 + (\kappa_1 M^2 / Rm) - \lambda_1^2 F}{\lambda_1^2 - \lambda_2^2} \right]$$

$$A_3 = \left[ \frac{F \lambda^2 - 1 - (\kappa_2 M^2 / Rm)}{2 \lambda \cosh \lambda} \right]$$

$$A_4 = \frac{\left[ 1 + (\kappa_2 M^2 / Rm) \right] \sin h \lambda - \lambda F (\lambda \sin h \lambda + 2 \cosh \lambda)}{2 \lambda \cosh^2 \lambda}$$

$$A_5 = \frac{\left[ 1 + (\kappa_3 M^2 / Rm) \right] \sin \lambda_3 \sinh \lambda_4 - F \left[ (\lambda_4^2 - \lambda_3^2) \sin \lambda_3 \sinh \lambda_4 + 2 \lambda_3 \lambda_4 \cos \lambda_3 \cosh \lambda_4 \right]}{2 \lambda_3 \lambda_4 (\cos^2 \lambda_3 \cosh^2 \lambda_4 + \sin^2 \lambda_3 \sinh^2 \lambda_4)}$$

$$A_6 = \frac{\left[ -1 - (\kappa_3 M^2 / Rm) \right] \cos \lambda_3 \cosh \lambda_4 + F \left[ (\lambda_4^2 - \lambda_3^2) \cos \lambda_3 \cosh \lambda_4 - 2 \lambda_3 \lambda_4 \sin \lambda_3 \sinh \lambda_4 \right]}{2 \lambda_3 \lambda_4 (\cos^2 \lambda_3 \cosh^2 \lambda_4 + \sin^2 \lambda_3 \sinh^2 \lambda_4)}$$

$$A_7 = \frac{1}{\cosh \lambda_6} \left[ \frac{1 + (\kappa_4 M^2 / Rm) + \lambda_5^2 F}{\lambda_5^2 + \lambda_6^2} \right]$$

$$A_8 = \frac{1}{\cos \lambda_5} \left[ \frac{1 + (\kappa_4 M^2 / Rm) - \lambda_6^2 F}{\lambda_5^2 + \lambda_6^2} \right]$$

$$\left. \begin{matrix} \lambda_1 \\ \lambda_2 \end{matrix} \right\} = \left( \frac{M^2 \pm \sqrt{M^4 - 4Ra}}{2} \right)^{1/2}$$

$$\lambda = Ra^{1/4}$$

$$\left. \begin{matrix} \lambda_3 \\ \lambda_4 \end{matrix} \right\} = \frac{Ra^{1/4}}{\sqrt{2}} \left( 1 \pm \frac{M^2}{2Ra^{1/2}} \right)^{1/2}$$

$$\left. \begin{matrix} \lambda_5 \\ \lambda_6 \end{matrix} \right\} = \left( \frac{\sqrt{M^4 - 4Ra \pm M^2}}{2} \right)^{1/2}$$

$$\kappa_1 = \frac{\frac{\text{Pr}_m}{\text{Pr}} \left[ F(\lambda_1^2 - \lambda_2^2) + (F\lambda_2^2 - 1) \frac{\tanh \lambda_1}{\lambda_1} - (F\lambda_1^2 - 1) \frac{\tanh \lambda_2}{\lambda_2} \right]}{(\lambda_1^2 - \lambda_2^2) (1 + \phi_2) + M^2 \left( \frac{\tanh \lambda_1}{\lambda_1} - \frac{\tanh \lambda_2}{\lambda_2} \right)}$$

$$\kappa_2 = \frac{\frac{\text{Pr}_m}{\text{Pr}} \left[ F \left( 3 - \frac{3 \tanh \lambda}{\lambda} - \tanh^2 \lambda \right) - \frac{1}{\lambda^2} \left( 1 - \frac{\tanh \lambda}{\lambda} - \tanh^2 \lambda \right) \right]}{2(\phi_2 + 1) + \frac{M^2}{\lambda^2} \left( 1 - \frac{\tanh \lambda}{\lambda} - \tanh^2 \lambda \right)}$$

$$\begin{aligned} \kappa_3 = & \frac{\text{Pr}_m}{\text{Pr}} \left[ 2\lambda_3\lambda_4 F(\lambda_3^2 + \lambda_4^2) (\cos^2 \lambda_3 \cosh^2 \lambda_4 + \sin^2 \lambda_3 \sinh^2 \lambda_4) \right. \\ & + \frac{\lambda_3 \sinh 2\lambda_4 - \lambda_4 \sin 2\lambda_3}{2} - \frac{F}{2} (\lambda_4^2 - \lambda_3^2) (\lambda_3 \sinh 2\lambda_4 - \lambda_4 \sin 2\lambda_3) \\ & \left. - F\lambda_3\lambda_4 (\lambda_3 \sin 2\lambda_3 + \lambda_4 \sinh 2\lambda_4) \right] \left[ \frac{M^2}{2} (\lambda_4 \sin 2\lambda_3 - \lambda_3 \sinh 2\lambda_4) \right. \\ & \left. + 2\lambda_3\lambda_4 (1 + \phi_2) (\lambda_3^2 + \lambda_4^2) (\cos^2 \lambda_3 \cosh^2 \lambda_4 + \sin^2 \lambda_3 \sinh^2 \lambda_4) \right]^{-1} \end{aligned}$$

$$\kappa_4 = \frac{\frac{\text{Pr}_m}{\text{Pr}} \left\{ F - \left( \frac{1}{\lambda_5^2 - \lambda_6^2} \right) \left[ (1 + \lambda_5^2 F) \frac{\tanh \lambda_6}{\lambda_6} + (1 + \lambda_6^2 F) \frac{\tanh \lambda_5}{\lambda_5} \right] \right\}}{(1 + \phi_2) + \left( \frac{M^2}{\lambda_5^2 + \lambda_6^2} \right) \left( \frac{\tanh \lambda_6}{\lambda_6} - \frac{\tanh \lambda_5}{\lambda_5} \right)}$$

## APPENDIX C

Nonconducting Wall Case Results1. Detailed Solutions

$$\text{a. } \underline{(m\pi/2\gamma)^2 > \frac{M^2}{4} [(4Ra/M^4) - 1]:}$$

$$\theta_{m1}(\xi) = \theta_m^{(1)}(\xi) + \alpha_1 \cosh \omega_1 \xi + \alpha_2 \cosh \omega_2 \xi \quad (C1)$$

$$\text{b. } \underline{(m\pi/2\gamma)^2 = \frac{M^2}{4} [(4Ra/M^4) - 1] \text{ (defines } M_0\text{):}}$$

$$\theta_2(\xi) = \theta^{(2)}(\xi) + \alpha_3 \xi \sinh \omega_3 \xi + \alpha_4 \cosh \omega_3 \xi \quad (C2)$$

$$\text{c. } \underline{(m\pi/2\gamma)^2 < \frac{M}{4} [(4Ra/M^4) - 1]:}$$

$$\theta_{m3}(\xi) = \theta_m^{(3)}(\xi) + \alpha_5 \sin \omega_4 \xi \sinh \omega_5 \xi + \alpha_6 \cos \omega_4 \xi \cosh \omega_5 \xi \quad (C3)$$

where

$$\theta_m^{(i)}(\xi) = -\frac{a_m [1 - (m\pi/2\gamma)^2 F]}{Ra + (m\pi/2\gamma)^4} + \frac{2mp_i \pi M^2 / \gamma Rm}{M^2 (m\pi/2\gamma)^2 - Ra} \sinh [(m\pi/2\gamma) \xi] \quad (C4)$$

$$\text{d. } \underline{(m\pi/2\gamma)^2 > \frac{M^2}{4} [(4Ra/M^4) - 1]:}$$

$$\begin{aligned} U_{m1}(\xi) = & a_m \left\{ F + \frac{(m\pi/2\gamma)^2 [1 - (m\pi/2\gamma)^2 F]}{Ra + (m\pi/2\gamma)^4} \right\} \\ & + [\omega_1^2 - (m\pi/2\gamma)^2] (\alpha_1 \cosh \omega_1 \xi) \\ & + [\omega_2^2 - (m\pi/2\gamma)^2] (\alpha_2 \cosh \omega_2 \xi) \end{aligned} \quad (C5)$$

$$\begin{aligned} B_{m1}(\xi) = & \left[ \frac{-2p_1 Ra \sinh (m\pi \xi / 2\gamma)}{(Mm\pi/2\gamma)^2 - Ra} \right] - \omega_1 \alpha_1 Rm \sinh \omega_1 \xi \\ & - \omega_2 \alpha_2 Rm \sinh \omega_2 \xi \end{aligned} \quad (C6)$$



$$e. \quad \frac{(m\pi/2\gamma)^2}{4} = \frac{M^2}{4} [(4Ra/M^4) - 1] \text{ (defines } m_0 \text{):}$$

$$\begin{aligned} U_2(\zeta) = & a_m \left\{ F + \frac{(m\pi/2\gamma)^2 [1 - (m\pi/2\gamma)^2 F]}{Ra + (m\pi/2\gamma)^4} \right\} \\ & + \{\alpha_3[\omega_3^2 - (m^2\pi^2/4\gamma^2)] \zeta\} \sinh \omega_3 \zeta \\ & + \{\alpha_4[\omega_3^2 - (m^2\pi^2/4\gamma^2)] + 2\omega_3\alpha_3\} \cosh \omega_3 \zeta \end{aligned} \quad (C7)$$

$$\begin{aligned} B_2(\zeta) = & \left[ \frac{-2p_2 Ra \sinh(m\pi\zeta/2\gamma)}{(Mm\pi/2\gamma)^2 - Ra} \right] - Rm(\omega_3\alpha_3\zeta) \cosh \omega_3 \zeta \\ & - Rm(\omega_3\alpha_4 + \alpha_6) \sinh \omega_3 \zeta \end{aligned} \quad (C8)$$

$$f. \quad \frac{(m\pi/2\gamma)^2}{4} < \frac{M^2}{4} [(4Ra/M^4) - 1]:$$

$$\begin{aligned} U_{m3}(\zeta) = & a_m \left\{ F + \frac{(m\pi/2\gamma)^2 [1 - (m\pi/2\gamma)^2 F]}{Ra + (m\pi/2\gamma)^4} \right\} \\ & + \{\alpha_5[\omega_5^2 - \omega_4^2 - (m^2\pi^2/4\gamma^2)] - 2\alpha_6\omega_4\omega_5\} \sin \omega_4 \zeta \sinh \omega_5 \zeta \\ & + \{\alpha_6[\omega_5^2 - \omega_4^2 - (m^2\pi^2/4\gamma^2)] + 2\alpha_5\omega_4\omega_5\} \cos \omega_4 \zeta \cosh \omega_5 \zeta \end{aligned} \quad (C9)$$

$$\begin{aligned} B_{m3}(\zeta) = & \left[ \frac{-2p_3 Ra \sinh(m\pi/2\gamma)}{(Mm\pi/2\gamma)^2 - Ra} \right] - Rm[(\alpha_5\omega_4 + \alpha_6\omega_5) \cos \omega_4 \zeta \sinh \omega_5 \zeta \\ & + (\alpha_5\omega_5 - \alpha_6\omega_4) \sin \omega_4 \zeta \cosh \omega_5 \zeta] \end{aligned} \quad (C10)$$

## 2. Pressure-drop Parameter

$$\begin{aligned} \frac{1 + 1/\gamma}{G} = & \sum_{m=1}^{m < m_0} \left( \frac{1 - \cos m\pi}{m\pi} \right) \left\{ a_m \left[ F + \frac{(m\pi/2\gamma)^2 [1 - (m^2\pi^2 F/4\gamma^2)]}{Ra + (m\pi/2\gamma)^4} \right] + (\alpha_1/\omega_1) [\omega_1^2 - (m^2\pi^2/4\gamma^2)] \sinh \omega_1 \right. \\ & + (\alpha_2\omega_2) [\omega_2^2 - (m^2\pi^2/4\gamma^2)] \sinh \omega_2 \left. \right\} + \left\{ \frac{1 - \cos M\gamma[(4Ra/M^4) - 1]^{1/2}}{M\gamma(4Ra/M^4 - 1)^{1/2}} \right\} \\ & \left\{ a_m \left[ F + \frac{(m\pi/2\gamma)^2 [1 - (m^2\pi^2 F/4\gamma^2)]}{Ra + (m\pi/2\gamma)^4} \right] + (\alpha_3\omega_3) [\omega_3^2 - (m^2\pi^2/4\gamma^2)] (\omega_3 \cosh \omega_3 - \sinh \omega_3) \right. \\ & + [(\sinh \omega_3)/\omega_3] \left[ \alpha_4 \left( \omega_3^2 - \frac{(m^2\pi^2)}{4\gamma^2} \right) + 2\omega_3\alpha_3 \right] \left. \right\} + \sum_{m > m_0}^{\infty} \left( \frac{1 - \cos m\pi}{m\pi} \right) \\ & \left\{ a_m \left[ F + \frac{(m\pi/2\gamma)^2 [1 - (m^2\pi^2 F/4\gamma^2)]}{Ra + (m\pi/2\gamma)^4} \right] + \left( \frac{2\omega_4\omega_5}{\omega_4^2 + \omega_5^2} \right) [(\alpha_5\omega_4 - \alpha_6\omega_5) \sin \omega_4 \cosh \omega_5 \right. \right. \\ & + (\alpha_5\omega_5 + \alpha_6\omega_4) \cos \omega_4 \sinh \omega_5] + \left[ \frac{\omega_5^2 - \omega_4^2 - (m^2\pi^2/4\gamma^2)}{\omega_5^2 + \omega_4^2} \right] [(\alpha_5\omega_5 + \alpha_6\omega_4) \sin \omega_4 \cosh \omega_5 \\ & \left. \left. + (\alpha_6\omega_5 - \alpha_5\omega_4) \cos \omega_4 \sinh \omega_5] \right\} \end{aligned} \quad (C11)$$

### 3. Nusselt Number

$$\begin{aligned}
\frac{G(G-F)}{2Nu(1+1/\gamma)} = & \sum_{m=1}^{m_0} \left\{ \frac{a_m}{4} \left[ F + \frac{(m\pi/2\gamma)^2 [1 - (m^2\pi^2/4\gamma^2) F]}{(m\pi/2\gamma)^4 + Ra} \right] \left[ \frac{a_m [1 - (m^2\pi^2/4\gamma^2) F]}{(m\pi/2\gamma)^4 + Ra} - \frac{\alpha_1 \sinh \omega_1}{\omega_1} - \frac{\alpha_2 \sinh \omega_2}{\omega_2} \right] \right. \\
& + \frac{a_m [1 - (m^2\pi^2/4\gamma^2) F]}{4[(m\pi/2\gamma)^4 + Ra]} \left[ (\alpha_1/\omega_1) \left( \omega_1^2 - \frac{m^2\pi^2}{4\gamma^2} \right) \sinh \omega_1 + (\alpha_2/\omega_2) \left( \omega_2^2 - \frac{m^2\pi^2}{4\gamma^2} \right) \sinh \omega_2 \right] \\
& + \frac{\alpha_1 \alpha_2 [\omega_1^2 + \omega_2^2 - (m^2\pi^2/2\gamma^2)]}{4(\omega_1^2 - \omega_2^2)} (\omega_2 \sinh \omega_2 \cosh \omega_1 - \omega_1 \sinh \omega_1 \cosh \omega_2) \\
& - \frac{\alpha_1^2}{8} \left[ \omega_1^2 - (m^2\pi^2/4\gamma^2) \right] \left( 1 + \frac{\sinh 2\omega_1}{2\omega_1} \right) + \frac{\alpha_2^2}{8} \left[ \omega_2^2 - m^2\pi^2/4\gamma^2 \right] \left( 1 + \frac{\sinh 2\omega_2}{2\omega_2} \right) \Big\} \\
& + \frac{a_{m_0}}{4} \left[ F + \frac{(m_0\pi/2\gamma)^2 [1 - (m_0^2\pi^2/4\gamma^2) F]}{(m_0\pi/2\gamma)^4 + Ra} \right] \left[ \frac{2a_{m_0} [1 - (m_0^2\pi^2/4\gamma^2) F]}{(m_0\pi/2\gamma)^2 + Ra} - \frac{\alpha_3 \cosh \omega_3}{\omega_3} + (\alpha_3/\omega_3 - \alpha_4) \frac{\sinh \omega_3}{\omega_3} \right] \\
& + \frac{a_{m_0} [1 - (m_0^2\pi^2/4\gamma^2) F]}{4\omega_3 [(m_0\pi/2\gamma)^4 + Ra]} \left\{ \left[ \alpha_3 \cosh \omega_3 - \left( \frac{\alpha_3}{\omega_3} - \alpha_4 \right) \sinh \omega_3 \right] \left( \omega_3^2 - \frac{m_0^2\pi^2}{4\gamma^2} \right) + 2\omega_3 \alpha_3 \sinh \omega_3 \right\} \\
& + (\alpha_3/32\omega_3^2) (2\omega_3 \cosh 2\omega_3 - \sinh 2\omega_3) \{ [\omega_3^2 - (m_0^2\pi^2/4\gamma^2) (\alpha_3 - 2\alpha_4) - 2\omega_3 \alpha_3] \\
& - \frac{\alpha_4}{8} [\alpha_4 \omega_3^2 - (m_0^2\pi^2/4\gamma^2)] + 2\alpha_3 \omega_4 \} \left( 1 + \frac{\sinh 2\omega_3}{2\omega_3} \right) + \frac{\alpha_3^2}{8} [\omega_3^2 - (m_0^2\pi^2/4\gamma^2)] \left( 1/3 - \frac{\sinh 2\omega_3}{2\omega_3} \right) \\
& + \sum_{m>m_0}^{\infty} \left\{ \frac{a_m}{4} \left[ F + \frac{(m\pi/2\gamma)^2 [1 - (m^2\pi^2/4\gamma^2) F]}{(m\pi/2\gamma)^4 + Ra} \right] \left[ \frac{a_m [1 - (m^2\pi^2/4\gamma^2) F]}{(m\pi/2\gamma)^4 + Ra} \right. \right. \\
& + \left. \left. \left( \frac{1}{\omega_4^2 + \omega_5^2} \right) [(\alpha_5 \omega_5 + \alpha_6 \omega_4) \sin \omega_4 \cosh \omega_5 + (\alpha_6 \omega_5 - \alpha_5 \omega_4) \cos \omega_4 \sinh \omega_5] \right\} \right. \\
& + \frac{a_m [1 - (m^2\pi^2/4\gamma^2) F]}{4(\omega_4^2 + \omega_5^2) [(m\pi/2\gamma)^4 + Ra]} \left\{ \left[ (\alpha_5 \omega_5 + \alpha_6 \omega_4) \left( \omega_5^2 - \omega_4^2 - \frac{m^2\pi^2}{4\gamma^2} \right) - 2\alpha_5 \omega_4 \omega_5 (\omega_5 - \omega_4) \right] \right. \\
& \sin \omega_4 \cosh \omega_5 + \left[ (\alpha_6 \omega_5 - \alpha_5 \omega_4) \left( \omega_5^2 - \omega_4^2 - \frac{m^2\pi^2}{4\gamma^2} \right) + 2\alpha_5 \omega_4 \omega_5 (\omega_4 + \omega_5) \right] \cos \omega_4 \sinh \omega_5 \Big\} \\
& + 2\alpha_5 \alpha_6 \omega_4 \omega_5 + \frac{1}{2} [\omega_5^2 - \omega_4^2 - (m^2\pi^2/4\gamma^2)] \left[ (\alpha_5^2 + \alpha_6^2) \left( \frac{\sin 2\omega_4}{2\omega_4} + \frac{\sinh 2\omega_5}{2\omega_5} \right) - (\alpha_5^2 - \alpha_6^2) \right] \\
& + \left( \frac{1}{\omega_4^2 + \omega_5^2} \right) \left\{ [\omega_5^2 - \omega_4^2 - (m^2\pi^2/4\gamma^2)] [\alpha_5 \alpha_6 \omega_5 + (\omega_4/4) (\alpha_5^2 + \alpha_6^2)] \sin 2\omega_4 \cosh 2\omega_5 \right. \\
& + \left. \left[ (1/4) (\alpha_5^2 + \alpha_6^2) \left( \omega_5^2 - \omega_4^2 - \frac{m^2\pi^2}{4\gamma^2} \right) - \omega_4^2 (\alpha_5^2 - \alpha_6^2) \right] \omega_5 \cos 2\omega_4 \sinh 2\omega_5 \right\} \Big\} \quad (C12)
\end{aligned}$$

#### 4. Integration Constants

$$\left. \begin{matrix} \omega_4 \\ \omega_2 \end{matrix} \right\} = \frac{1}{\sqrt{2}} \left\{ M^2 + 2(m\pi/2\gamma)^2 \pm [M^4 + 4M^2(m\pi/2\gamma)^2 - 4Ra]^{1/2} \right\}^{1/2}$$

$$\omega_3 = \frac{M}{2} [1 + (4Ra/M^4)]^{1/2}$$

$$\left. \begin{matrix} \omega_4 \\ \omega_5 \end{matrix} \right\} = \frac{1}{2} \left\{ 2[Ra + (m\pi/2\gamma)^4]^{1/2} \pm M^2 \pm 2(m\pi/2\gamma)^2 \right\}^{1/2}$$

$$\alpha_1 = \frac{1}{(\omega_2^2 - \omega_1^2) \cosh \omega_1} \left\{ -2p_1[\omega_2^2 - (m\pi/2\gamma)^2] \left[ \frac{(M^2 m\pi/2\gamma Rm)}{(Mm\pi/2\gamma)^2 - Ra} \right] \cosh \left( \frac{m\pi}{2\gamma} \right) \right. \\ \left. + a_m F + \frac{a_m \omega_2^2}{Ra + (m\pi/2\gamma)^4} [1 - F(m\pi/2\gamma)^2] \right\}$$

$$\alpha_2 = \frac{1}{(\omega_2^2 - \omega_1^2) \cosh \omega_2} \left\{ 2p_1[\omega_1^2 - (m\pi/2\gamma)^2] \left[ \frac{(M^2 m\pi/2\gamma Rm)}{(Mm\pi/2\gamma)^2 - Ra} \right] \cosh \left( \frac{m\pi}{2\gamma} \right) \right. \\ \left. - a_m F - \frac{a_m \omega_1^2}{Ra + (m\pi/2\gamma)^4} [1 - F(m\pi/2\gamma)^2] \right\}$$

$$\alpha_3 = \frac{1}{2\omega_3 \cosh \omega_3} \left\{ 2p_2[\omega_3^2 - (m\pi/2\gamma)^2] \left[ \frac{(M^2 m\pi/2\gamma Rm)}{(Mm\pi/2\gamma)^2 - Ra} \right] \cosh (m\pi/2\gamma) \right. \\ \left. - a_m F - \frac{a_m \omega_3^2}{Ra + (m\pi/2\gamma)^4} [1 - F(m\pi/2\gamma)^2] \right\}$$

$$\alpha_4 = \frac{1}{2\omega_3 \cosh \omega_3} \left\{ -2p_2 \left[ \left( \omega_3^2 - \frac{m^2 \pi^2}{4\gamma^2} \right) \tanh \omega_3 + 2\omega_3 \right] \right. \\ \left[ \frac{(M^2 m\pi/2\gamma Rm)}{(Mm\pi/2\gamma)^2 - Ra} \right] \cosh (m\pi/2\gamma) + a_m F \tanh \omega_3 \\ \left. + \frac{a_m (\omega_3^2 \tanh \omega_3 + 2\omega_3)}{Ra + (m\pi/2\gamma)^4} [1 - F(m\pi/2\gamma)^2] \right\}$$

$$\alpha_5 = \frac{1}{2\omega_4\omega_5(\cos^2 \omega_4 \cosh^2 \omega_5 + \sin^2 \omega_4 \sinh^2 \omega_5)} \left\{ 2p_3 \left[ \frac{(M^2 m \pi / 2 \gamma R m)}{(M m \pi / 2 \gamma)^2 - R a} \right] \right. \\ \left[ \left( \omega_5^2 - \omega_4^2 - \frac{m^2 \pi^2}{4 \gamma^2} \right) \cos \omega_4 \cosh \omega_5 - 2 \omega_4 \omega_5 \sin \omega_4 \sinh \omega_5 \right] \cosh (m \pi / 2 \gamma) \\ \left. + \frac{a_m [1 - F(m \pi / 2 \gamma)^2]}{R a + (m \pi / 2 \gamma)^4} [2 \omega_4 \omega_5 \sin \omega_4 \sinh \omega_5 - (\omega_5^2 - \omega_4^2) \cos \omega_4 \cosh \omega_5] \right\}$$

$$\alpha_6 = \frac{1}{2\omega_4\omega_5(\cos^2 \omega_4 \cosh^2 \omega_5 + \sin^2 \omega_4 \sinh^2 \omega_5)} \left\{ -2p_3 \left[ \frac{(M m \pi / 2 \gamma R m)}{(M m \pi / 2 \gamma)^2 - R a} \right] \right. \\ \left[ \left( \omega_5^2 - \omega_4^2 - \frac{m^2 \pi^2}{4 \gamma^2} \right) \sin \omega_4 \sinh \omega_5 + 2 \omega_4 \omega_5 \cos \omega_4 \cosh \omega_5 \right] \cosh (m \pi / 2 \gamma) \\ \left. + \frac{a_m [1 - F(m \pi / 2 \gamma)^2]}{R a + (m \pi / 2 \gamma)^4} [2 \omega_4 \omega_5 \cos \omega_4 \cosh \omega_5 + (\omega_5^2 - \omega_4^2) \sin \omega_4 \sinh \omega_5] \right\}$$

$$p_1 = -q_1 = \frac{a_m R m [(M m \pi / 2 \gamma)^2 - R a]}{2(\omega_2^2 - \omega_1^2)} \left\{ (\omega_1 \tanh \omega_1 - \omega_2 \tanh \omega_2) F \right. \\ \left. + \omega_1 \omega_2 [1 - F(m \pi / 2 \gamma)^2] \left[ \frac{\omega_2 \tanh \omega_1 - \omega_1 \tanh \omega_2}{R a + (m \pi / 2 \gamma)^4} \right] \right\} / \left\{ -R a \sinh (m \pi / 2 \gamma) \right. \\ \left. + [(M m \pi / 2 \gamma)^2 \cosh (m \pi / 2 \gamma)] \left[ \frac{\omega_1 [\omega_2^2 - (m^2 \pi^2 / 4 \gamma^2)] \tanh \omega_1 - \omega_2 [\omega_1^2 - (m^2 \pi^2 / 4 \gamma^2)] \tanh \omega_2}{\omega_2^2 - \omega_1^2} \right] \right\}$$

$$p_2 = -q_2 = (a_m R m / 4) [(M m \pi / 2 \gamma)^2 - R a] \left\{ 1 - \tanh^2 \omega_3 + \frac{\tanh \omega_3}{\omega_3} + \left[ \frac{1 - F(m \pi / 2 \gamma)^2}{R a + (m \pi / 2 \gamma)^4} \right] [\omega_3^2 + \omega_3] \right. \\ \left. - (\omega_3^2 \tanh \omega_3 + 2 \omega_3 \tanh \omega_3) \right\} / \left\{ R a \sinh (m \pi / 2 \gamma) \right. \\ \left. + (M m \pi / 2 \gamma)^2 \frac{1}{2} \cosh (m \pi / 2 \gamma) \left[ (\omega_3^2 - m^2 \pi^2 / 4 \gamma^2) \left( 1 + \tanh^2 \omega_3 - \frac{\tanh \omega_3}{\omega_3} \right) + 2 \omega_3 \tanh \omega_3 \right] \right\}$$

$$p_3 = -q_3 = \left[ \frac{a_m R m [1 - F(m^2 \pi^2 / 4 \gamma^2)] (M^2 m^2 \pi^2 / 4 \gamma^2 - R a)}{R a + (m \pi / 2 \gamma)^4} \right] \left[ \frac{(\omega_5^2 - \omega_4^2) \left( \frac{\sinh 2 \omega_5}{2 \omega_5} + \frac{\sin 2 \omega_4}{2 \omega_4} \right)}{2 \omega_5} \right. \\ \left. - (\omega_5 \sinh 2 \omega_5 - \omega_4 \sin 2 \omega_4) \right] \left\{ 4 R a (\cos^2 \omega_4 \cosh^2 \omega_5 + \sin^2 \omega_4 \sinh^2 \omega_5) \sinh (m \pi / 2 \gamma) \right. \\ \left. + 2 M^2 (m \pi / 2 \gamma) \sinh (m \pi / 2 \gamma) \left[ -(\omega_5 \sinh 2 \omega_5 - \omega_4 \sin 2 \omega_4) \right. \right. \\ \left. \left. + [\omega_5^2 - \omega_4^2 - (m^2 \pi^2 / 4 \gamma^2)] \left( \frac{\sinh 2 \omega_5}{2 \omega_5} + \frac{\sin 2 \omega_4}{2 \omega_4} \right) \right] \right\}^{-1}$$

## ACKNOWLEDGMENTS

I would like to acknowledge the work of Irene Baksys and Millie Schlapkohl of the Applied Mathematics Division of Argonne National Laboratory in programing an IBM-704 digital computer to perform the many computations presented in this report. I would also like to acknowledge the work done by Arthur Wright in checking the many algebraic manipulations.

## REFERENCES

1. Hartmann, J., Hg-Dynamics I, Theory of the Laminar Flow of an Electrically Conductive Liquid in a Homogeneous Magnetic Field, Kgl. Danske Videnskab. Selskab, Mat.-Fys. Medd. 15, No. 6 (1937).
2. Shercliff, J. A., Steady Motion of Conducting Fluids in Pipes under Transverse Magnetic Fields, Proc. Cambridge Phil. Soc. 49 (1953), 136-144.
3. Shercliff, J. A., The Flow of Conducting Fluids in Circular Pipes under Transverse Magnetic Fields, J. Fluid Mech. 1 (1956), 644-666.
4. Uflyand, Ya. S., Flow Stability of a Conducting Fluid in a Rectangular Channel in a Transverse Magnetic Field, Soviet Phys. - Tech. Phys. 5 (1960), 1191-1193.
5. Chekmarev, I. B., Nonstationary Flow of a Conducting Fluid in a Flat Tube in the Presence of a Transverse Magnetic Field, Soviet Phys. - Tech. Phys. 5 (1960), 313-319.
6. Chang, C. C., and T. S. Lundgren, The Flow of an Electrically Conducting Fluid through a Duct with Transverse Magnetic Field, Proc. 1959 Heat Transf. Fluid Mech. Inst., 41-54.
7. Chang, C. C., and T. S. Lundgren, Duct Flow in Magnetohydrodynamics, Z. Angew. Math. u. Phys. 12 (1961), 100-114.
8. Chang, C. C., and J. T. Yen, Magnetohydrodynamic Channel Flow as Influenced by Wall Conductance, Z. Angew. Math. u. Phys. 13 (1962), 266-272.
9. Yen, J. T., Effect of Wall Electrical Conductance on Magnetohydrodynamic Heat Transfer in a Channel, ASME Paper No. 62-WA-171 (1962).
10. Smirnov, A. G., The Theory of Certain Magnetohydrodynamic Phenomena Occurring in the Free Laminar Thermal Convection of the Electrically Conducting Fluid in a Round Vertical Pipe Located in a Weak Magnetic Field, Soviet Phys. - Tech. Phys. 4 (1959), 1141-1147.
11. Poots, G., Laminar Natural Convection Flow in Magnetohydrodynamics, Int. J. Heat Mass Transfer 3 (1961), 1-25.
12. Osterle, J. F., and F. J. Young, Natural Convection between Heated Vertical Plates in a Horizontal Magnetic Field, J. Fluid Mech. 11 (1961), 512-518.
13. Mori, Y., On Combined Free and Forced Convective Laminar Magnetohydrodynamic Flow and Heat Transfer in Channels with Transverse Magnetic Field, Intl. Devel. Heat Transfer, Part V (1961), 1031-1037.

14. Regirer, S. A., On Convective Motion of a Conducting Fluid between Parallel Vertical Plates in a Magnetic Field, Zh. Eksper. i Teoret. Fiz. 37 (1959), 212-216.
15. Regirer, S. A., Magnetohydrodynamic Problems of Stabilized Convection in Vertical Channels, Zh. Prek. Mekh. i Tekh. Fiz. 1 (1962), 15-19.
16. Alpher, R. A., Heat Transfer in Magnetohydrodynamic Flow between Parallel Plates, Intl. J. Heat Mass Transfer 3 (1961), 108-112.
17. Perlmutter, M., and R. Siegel, Heat Transfer to an Electrically Conducting Fluid Flowing in a Channel with a Transverse Magnetic Field, NASA TN D-875 (1961).
18. Shohet, J. L., Velocity and Temperature Profiles for Laminar Magnetohydrodynamic Flow in the Entrance Region of an Annular Channel, Phys. Fluids 5 (1962), 879-884.
19. Globe, S., Laminar Steady-state Magnetohydrodynamic Flow in an Annular Channel, Phys. Fluids 2 (1959), 404-407.
20. Cambel, A. B., Plasma Physics and Magnetofluidmechanics, McGraw-Hill Book Company, New York (1963), 32-55.
21. Elsasser, W. M., Dimensional Reactions in Magnetohydrodynamics, Phys. Rev. 95 (1954), 1-5.
22. Ostrach, S., Combined Natural- and Forced-convection Laminar Flow and Heat Transfer of Fluids with and without Heat Sources in Channels with Linearly Varying Wall Temperatures, NACA TN 3141 (1954).
23. Ryabinin, A. G., and A. I. Khozhainov, Steady-state Laminar Flow of an Electrically Conducting Fluid in a Rectangular Tube under the Action of Ponderomotive Forces, Soviet Phys. - Tech. Phys. 7 (1962), 9-13.
24. Han, L. S., Laminar Heat Transfer in Rectangular Channels, Trans. ASME 81, Series C, J. Heat Transfer (1959), 121-128.
25. Churchill, R. V., Operational Mathematics, 2nd ed., McGraw-Hill Book Company, New York (1958), 288-320.



ARGONNE NATIONAL LAB WEST



3 4444 00008186 9

✂